The Canadian Journal of Chemical Engineering

THE UNIVERSITY OF MICHIGAN
SEP 6 1961
ENGINEERING LIBRARY

formerly

CANADIAN JOURNAL OF TECHNOLOGY

CONTENTS

Taylor Diffusion in Tubular Reactors — *Joseph Coste, Dale Rudd, Neal R. Amundson* — **149**

Mass Transfer With and Without Chemical Reaction — *J. Marangozis, A. I. Johnson* — **152**

High Speed Photography in the Study of Two-Phase Flow — *R. A. S. Brown, G. W. Govier* — **159**

Determination of Ternary Liquid-Liquid Systems by Use of the Lever Rule — *E. L. Heric, Kenneth R. Williams* — **165**

Note to the Editor

A Generalized Method for the Estimation of Heat of Vaporization — *Carl St. Pierre, Chi Tien* — **170**

Industrial Section

Pilot Plant Unit for the Continuous Methanolysis of Glyceride Oils — *P. M. Janguaard, F. A. Vandenheuvel* — **172**

Safety of Materials of Construction Used in Explosives Manufacture — *F. Van Zeggeren* — **175**

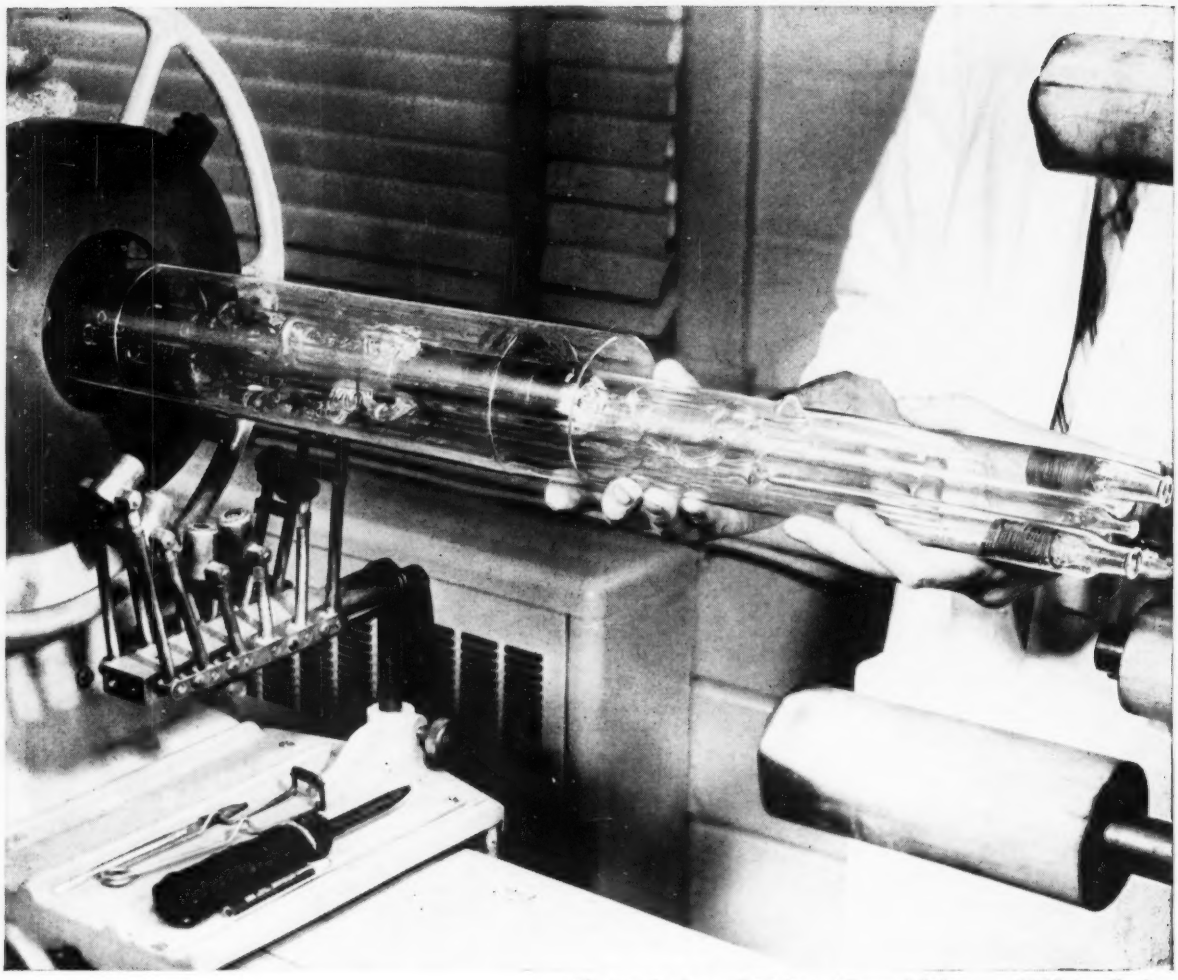

Photograph taken at C-I-L Central Research Laboratory, McMasterville, Que.

POLYMERIC PRECISION

This is an ebulliometer—being assembled by the master glass-blower on his own lathe at our Central Research Laboratory.

The ebulliometer uses two vapor lift pumps such as those found in electric coffee percolators. One circulates a polymer solution while the other circulates boiling solvent—each liquid stream is directed over a temperature detector so sensitive that a difference of one-millionth of 1°C. may be sensed. This device allows the measurement of high molecular weights related to the physical properties of polymers.

Such C-I-L research contributes to higher standards of performance in the plastics industry . . . to new and better plastic products . . . and—through better technical service—to greater success in the application of these new materials to modern living.

C-I-L

CANADIAN INDUSTRIES LIMITED

Serving Canadians Through Chemistry

Agricultural Chemicals • Ammunition • Coated Fabrics • Industrial Chemicals • Commercial Explosives • Paints • Plastics • Textile Fibres

The Canadian Journal of Chemical Engineering

formerly

Canadian Journal of Technology

Published by The Chemical Institute of Canada

VOLUME 39 | AUGUST, 1961 | NUMBER 4

Editor
A. Cholette
Faculty of Science, Laval University
Quebec, Que.

Managing Editor
T. H. G. Michael

Publishing Editor
D. W. Emmerson

Assistant Publishing Editors
R. G. Watson
R. N. Callaghan

Circulation Manager
M. M. Lockey

EDITORIAL BOARD

Chairman
L. D. DOUGAN, Polymer Corp. Limited, Sarnia, Ont.

P. W. BLAYLOCK, Shawinigan Chemicals Limited, Montreal, Que.

W. M. CAMPBELL, Atomic Energy of Canada Limited, Chalk River, Ont.

F. A. FORWARD, University of British Columbia, Vancouver, B.C.

J. W. HODGINS, McMaster University, Hamilton, Ont.

A. I. JOHNSON, University of Toronto, Toronto, Ont.

R. R. McLAUGHLIN, University of Toronto, Toronto, Ont.

G. L. OSBERG, National Research Council, Ottawa, Ont.

A. C. PLEWES, Queen's University, Kingston, Ont.

L. W. SHEMILT, University of New Brunswick, Fredericton, N.B.

J. H. SHIPLEY, Canadian Industries Limited, Montreal, Que.

H. R. L. STREIGHT, Du Pont of Canada Limited, Montreal, Que.

EX-OFFICIO

LEO MARION, President, The Chemical Institute of Canada.

LEO YAFFE, Chairman of the Board of Directors.

J. H. SHIPLEY, Director of Publications.

Authorized as second class mail, Post Office Department, Ottawa. Printed in Canada

Manuscripts for publication should be submitted to the Editor: Dr. A. Cholette, Faculty of Science, Laval University, Boulevard de l'Entente, Quebec, Que. (Instructions to authors are on the next page).

Editorial, Production and Circulation Offices: 48 Rideau Street, Ottawa 2, Ont.

Advertising Office: C. N. McCuaig, manager of advertising sales, *The Canadian Journal of Chemical Engineering*, Room 601, 217 Bay Street, Toronto, Ont. Telephone—EMpire 3-3871.

Plates and Advertising Copy: Send to *The Canadian Journal of Chemical Engineering*, 48 Rideau Street, Ottawa 2, Ont.

Subscription Rates: In Canada—$6.00 per year and $1.25 per single copy; U.S. and U.K.—$7.00, Foreign—$7.50.

Change of Address: Advise Circulation Department in advance of change of address, providing old as well as new address. Enclose address label if possible.

The Canadian Journal of Chemical Engineering is published by The Chemical Institute of Canada every two months.

Unless it is specifically stated to the contrary, the Institute assumes no responsibility for the statements and opinions expressed in *The Canadian Journal of Chemical Engineering*. Views expressed in the editorials do not necessarily represent the official position of the Institute.

The Canadian Journal of Chemical Engineering

INSTRUCTIONS TO AUTHORS

Manuscript Requirements for Articles

1. The manuscript should be in English or French.
2. The original and two copies of the manuscript should be supplied. These are to be on 8½ x 11 inch sheets, typewritten, and double spaced. Each page should be numbered.
3. Symbols should conform to American Standards Association. An abridged set of acceptable symbols is found in the third edition of Perry's Chemical Engineers' Handbook. Greek letters and subscripts and superscripts should be carefully made.
4. Abstracts of not more than 200 words in English indicating the scope of the work and the principal findings should accompany all technical papers.
5. References should be listed in the order in which they occur in the paper, after the text, using the form shown here: "Othmer, D. F., Jacobs, Jr., J. J., and Levy, J. F., Ind. Eng. Chem. **34**, 286 (1942). Abbreviations of journal names should conform to the "List of Periodicals Abstracted by Chemical Abstracts". Abbreviations of the common journals are to be found in Perry's Handbook also. All references should be carefully checked with the original article.
6. Tables should be numbered in Arabic numerals. They should have brief descriptive titles and should be appended to the paper. Column headings should be brief. Tables should contain a minimum of descriptive material.
7. All figures should be numbered from 1 up, in Arabic numerals. Drawings should be carefully made with India ink on white drawing paper or tracing linen. All lines should be of sufficient thickness to reproduce well, especially if the figure is to be reduced. Letters and numerals should be carefully and neatly made, with a stencil. Generally speaking, originals should not be more than twice the size of the desired reproduction; final engravings being 3¼ in. or 7 in. wide depending on whether one column or two is used. For further details ask the Editor for the Guide for Drawings.
8. Photographs should be made on glossy paper with strong contrasts. Photographs or groups of photographs should not be larger than three times the size of the desired reproduction.
9. All tables and figures should be referred to in the text.

Submission of Manuscripts

1. The three copies of the manuscript, including figures and tables, should be sent directly to:
   DR. A. CHOLETTE, editor,
   The Canadian Journal of Chemical Engineering,
   Faculty of Science, Laval University,
   Boulevard de l'Entente,
   Quebec, Que.
2. The authors addresses and titles should be submitted with the manuscript.
3. The author may suggest names of reviewers for his article, but the selection of the reviewers will be the responsibility of the editor. Each paper or article is to be reviewed by two chemical engineers familiar with the topic. Reviewers will remain anonymous.
4. All correspondence regarding reviews should be directed to the editor.

Reprints

1. At least 50 free "tear sheets" of each paper will be supplied.
2. Additional reprints may be purchased at cost. An estimated cost of reprints, with an attached order form, will be sent to the author with the galley proofs.
3. Orders for reprints must be made before the paper has appeared in the Journal.

Communications, Letters and Notes to the Editor

Short papers, as described below, will be considered for publication in this Journal. Their total length should be such that they will not occupy more than one page of the Journal.

Communications

A communication is a prompt preliminary report of observations made which are judged to be sufficiently important to warrant expedited publication. It usually calls for a more expanded paper in which the original matter is republished with more details.

Letters

A letter consists of comments or remarks submitted by readers or authors in connection with previously published material. It may deal with various forms of discussion arising out of a publication or it may simply report and correct inadvertent errors.

Notes

A note is a short paper which describes a piece of work not sufficiently important or complete to make it worth a full article. It may refer to a study or piece of research which, while it is not finished and may not be finished, offers interesting aspects or facts. As in the case of an article a note is a final publication.

* * *

Taylor Diffusion in Tubular Reactors[1]

JOSEPH COSTE[2], DALE RUDD[3] and NEAL R. AMUNDSON[4]

In order to estimate the effect of velocity profile and radial diffusion on conversion in tubular reactors the assumption of Taylor diffusion is adopted. This leads to equations which are simple, but because of the numerical instability of these equations they are approximated to by a cell model in order to obtain numerical results. It is shown that the cell model can be a very good approximation to the one dimensional diffusion equation. If the Taylor diffusion model is valid for systems involving chemical reaction and heat transfer it may be concluded that while there seem to be no gross effects in a tubular turbulent reactor there are differences in detail, such as maximum temperature at the hot spot, which may be important.

In order to solve the problem of a tubular reactor to determine the conversion and heat transfer characteristics it is necessary to consider a rather complicated system of partial differential equations. This system is complicated because the velocity profile is not flat and because there are gradients of concentration, temperature, and pressure. To solve this problem in a general way analytically is, of course, out of the question and the numerical solution is tedious and requires a very large computer. At the same time there is the larger question whether from a practical point of view the effects mentioned above are important enough to justify the effort needed to solve the problem. It would be interesting, however, to obtain some estimate of the magnitude of some of these effects, and it is the purpose of this paper to exploit a technique which might give a partial insight into the problem.

G. I. Taylor[1,2] and later Sjenitzer[3] and Tichacek, Barkelew, and Baron[4] showed that the effect of nonflat velocity profile and radial mixing under the assumption of the Reynolds' analogy could be combined into a single parameter, a quasi longitudinal mixing coefficient which appears in the differential equations as a diffusivity. This has the advantage that the partial differential equation is replaced by an ordinary differential equation whose solution is more tractable. The above mentioned authors considered the problem in which only two modes of transport were important, that by the non-flat profile which causes gradients of concentration and the resultant transport by radial diffusion caused by the gradients set up by the profile. Other modes of transport were considered to be negligible compared with these. Taylor showed that in laminar flow the proper quasi longitudinal diffusion coefficient was

$$D^* = \frac{a^2 V^2}{48D}$$

where D is the molecular diffusivity, while for turbulent flow

$$D^* = 10.1 a V \sqrt{\frac{\tau}{\rho V^2}}$$

where $\sqrt{\tau/\rho V^2}$ is a dimensionless friction factor.

The basic assumption of this paper is that the quasi mixing coefficient of Taylor may be used in the tubular reactor in which chemical reaction, heat transfer, and diffusion are coupled. While it is undoubtedly true that the assumptions under which Taylor diffusion was derived are not valid in this case, it is hoped that an estimate of the effect of profile and radial diffusion might be obtained for comparison with the lumped constant reactor.

General Problem

For the purposes of this paper an incompressible fluid with a single irreversible first order exothermic reaction will be considered. If c is the concentration of reactant then the mass conservation equation with Taylor diffusion is

$$D^* \frac{d^2c}{dx^2} - V\frac{dc}{dx} = cp\, e^{-\frac{E}{RT}} \qquad (1)$$

where V is the average velocity of the turbulent flow field. The equation of energy conservation with the usual simplifying assumptions is

$$D^* \frac{d^2T}{dx^2} - V\frac{dT}{dx} + K(T_w - T) = -cp\, e^{-\frac{E}{RT}} Q \qquad (2)$$

where the Reynolds analogy is assumed to hold. With these equations must be associated some inlet conditions. For our purposes the following will be used,

$$Vc_{in} = Vc - D^*\frac{dc}{dx};\ x = 0$$

$$VT_{in} = VT - D^*\frac{dT}{dx};\ x = 0$$

It is convenient to make the change of variable $v = x/V$ to give

$$\frac{D^*}{V^2}\frac{d^2c}{dv^2} - \frac{dc}{dv} = cp\, e^{-\frac{E}{RT}} \qquad (3)$$

$$\frac{D^*}{V^2}\frac{d^2T}{dv^2} - \frac{dT}{dv} + K(T_w - T) = -cp\, e^{-\frac{E}{RT}} Q \qquad (4)$$

$$c_{in} = c - \frac{D^*}{V^2}\frac{dc}{dv} \qquad (5)$$

$$T_{in} = T - \frac{D^*}{V^2}\frac{dT}{dv} \qquad (6)$$

where the variable v is a residence time. Another condition must be stated to completely specify the solution. It will be assumed that the reactor is long enough that a finiteness condition may be imposed on all solutions.

[1]*Manuscript received January 28; accepted May 3, 1961.*
[2]*French Army.*
[3]*Department of Chemical Engineering, University of Wisconsin, Madison, Wis., U.S.A.*
[4]*University of Minnesota, Minneapolis, Minn., U.S.A.*
Contribution from the University of Minnesota, Minneapolis, Minn., U.S.A.

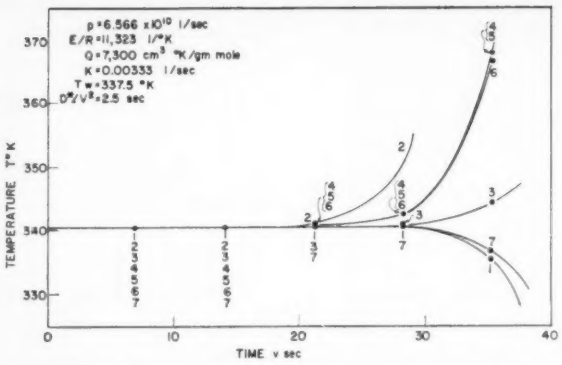

Figure 1—Sequence of forward integration attempts of the diffusion equations : temperature.

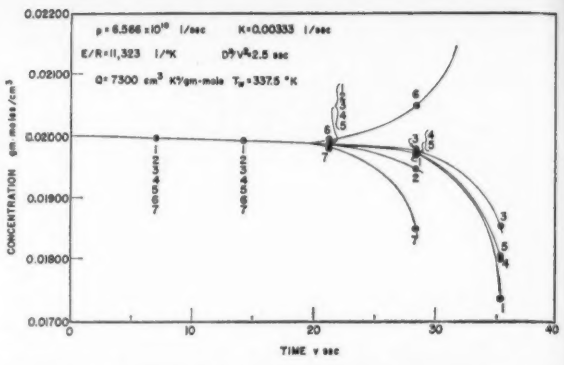

Figure 2—Sequence of forward integration attempts of the diffusion equations : concentrations.

Equations (3), (4), (5), and (6) will be solved by the marching technique, that is, by starting at the reactor entrance and proceeding stepwise down the reactor. In order to initiate the calculations the values of dc/dv and dT/dv must be known at the entrance. These are unknown but a good approximation may be obtained from the solution of the same problem treated as a lumped constant system. Integrations were then performed using the Gill modification of the Runge-Kutta technique. It was found that there were no values of the gradients which would produce finite solutions. A change of a single unit in the sixth significant figure in the inlet gradient makes the solution change from large positive to large negative values as shown in Figures 1 and 2. Curves 1 thru 7 on these figures show the effect of progressively better estimates of the inlet gradients. It should be mentioned that the effect of increment size has presumably been removed from these calculations.

The phenomenon described above is not an unusual one and is discussed by Fox[6]. For linear equations the same phenomenon may exist since, in effect, one is trying to guess the inlet gradients which will give certain values to the arbitrary constants which appear in the general solution. For example, if one term of the solution becomes very large for large v then its coefficient must be exactly zero. In a computer with finite precision this may not be possible.

The possibility of integrating the equations in the reverse direction exists but in this case four values must be estimated, c, T, dc/dv, and dT/dv at some point. This does not seem feasible.

Finite Cell Model

One may imagine a tubular reactor divided into cells, each of which resembles a stirred pot, of length Δx. It is clear that in the limit as Δx approaches zero the series of stirred pots approach a tubular reactor with lumped parameters. On the other hand for a non-zero Δx the mixing in each of the cells produces an effect like that of axial mixing save for the fact there is no back mixing. The mass and energy conservation equations may be written as

$$V(T_{x-\Delta x} - T_x) = -c_x p\, e^{-\frac{E}{RT_x}} Q\, \Delta x + K(T_x - T_w)\, \Delta x$$

$$V(c_{x-\Delta x} - c_x) = c_x p\, e^{-\frac{E}{RT_x}} \Delta x$$

where the subscripts denote the cell in which the evaluation is to be made. Now if one desires the cell model and continuous model to agree the best in some sense one must have a criterion for the choice of Δx. One way to proceed is as follows. Let $T_{x-\Delta x}$ be expanded into Taylor series about T_x and choose Δx so that the two models agree through second order derivatives. Thus,

$$T_{x-\Delta x} = T_x - \Delta x \frac{dT}{dx} + \frac{\Delta x^2}{2'.} \frac{d^2T}{dx^2} + \cdots$$

$$c_{x-\Delta x} = c_x - \Delta x \frac{dc}{dx} + \frac{\Delta x^2}{2'.} \frac{d^2c}{dx^2} + \cdots$$

The discrete model then becomes

$$V\left[-\frac{dT}{dx} + \frac{d^2T}{dx^2}\frac{\Delta x}{2}\right] \simeq -c_x p\, e^{-\frac{E}{RT_x}} Q + K(T_x - T_w)$$

$$V\left[-\frac{dc}{dx} + \frac{d^2c}{dx^2}\frac{\Delta x}{2}\right] \simeq c_x p\, e^{-\frac{E}{RT_x}}$$

Comparison of these two equations with Equations (3) and (4) reveals that the equations will be identical through second derivative terms if

$$\frac{V\Delta x}{D^*} = 2$$

or

$$\frac{V^2\Delta v}{D^*} = 2$$

or

$$(\Delta x)^2 = 2D^*\Delta v$$

which bears a resemblance to the Einstein relation.

If we now think of $n\Delta x = x$, then

$$T_{n-1} = T_n - \frac{\Delta x}{V} p\, e^{-\frac{E}{RT_n}} c_n Q + \frac{\Delta x}{V} K(T_n - T_w) \quad \ldots\ldots\ldots (7)$$

$$c_{n-1} = c_n + \frac{\Delta x}{V} p\, e^{-\frac{E}{RT_n}} c_n$$

and the solution of these equations may be started by specifying $T_o = T_{in}$ and $c_o = c_{in}$. For more complicated kinetic relations Equations (7) and (8) would require some iterative approximate solution but for the case at hand Equation (8) may be solved for c_n, the latter substituted in Equation (7) with the solution for T_n following.

Two cases were computed and these are shown on Figures 3 and 4. The parameters for the system are given on the figures and the two graphs are for cases

$$\frac{\Delta x}{2V} = 5 \text{ sec. and } \frac{\Delta x}{2V} = 10 \text{ sec.}$$

where these would hold for a typical turbulent flow. The small circles represent the values of concentration and temperature versus residence time v. The curves which appear to

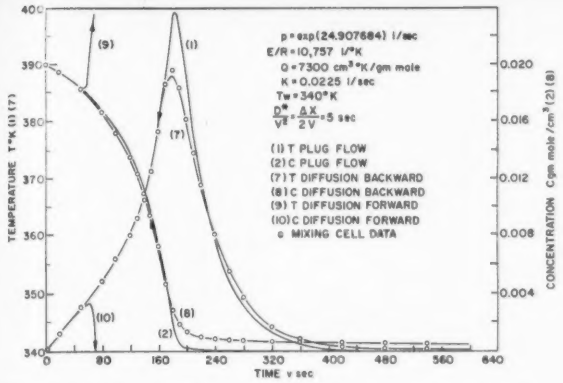
p = exp(24.907684) 1/sec
E/R = 10,757 1/°K
Q = 7300 cm³ °K/gm mole
K = 0.0225 1/sec
Tw = 340°K
D*/V² = Δx/2V = 5 sec
(1) T PLUG FLOW
(2) C PLUG FLOW
(7) T DIFFUSION BACKWARD
(8) C DIFFUSION BACKWARD
(9) T DIFFUSION FORWARD
(10) C DIFFUSION FORWARD
o MIXING CELL DATA
TEMPERATURE T °K (1) (7)
CONCENTRATION C gm mole/cm³ (2) (8)
TIME v sec

Figure 3—Mixing cell, backward integration and plug flow profiles. $D^*/V^2 = 5$.

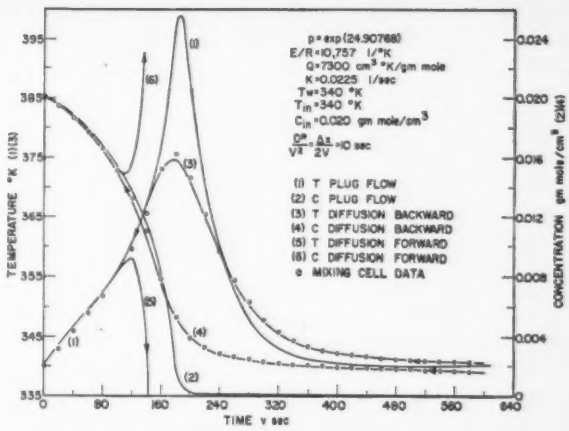
p = exp(24.90768)
E/R = 10,757 1/°K
Q = 7300 cm³ °K/gm mole
K = 0.0225 1/sec
Tw = 340 °K
Tin = 340 °K
Cin = 0.020 gm mole/cm³
D*/V² Δx/2V = 10 sec
(1) T PLUG FLOW
(2) C PLUG FLOW
(3) T DIFFUSION BACKWARD
(4) C DIFFUSION BACKWARD
(5) T DIFFUSION FORWARD
(6) C DIFFUSION FORWARD
o MIXING CELL DATA
TEMPERATURE °K (1)(3)
CONCENTRATION gm mole/cm³ (2)(4)
TIME v sec

Figure 4—Mixing cell, backward integration and plug flow profiles. $D/V^2 = 10$.

pass through these points are *not* smoothed curves. It is now possible to obtain estimates of the concentration, temperature, and their gradients for a large v and so integrate the differential equations, Equations (3) and (4), backwards. This was done by taking these values at $v = 600$ and the equations were integrated. The curves which appear to pass through the small circles were obtained and, further, the inlet conditions, Equations (5) and (6), were satisfied within a distance of one cell, which is all that one could expect. It is a remarkable fact that the mixing cell model and continuous model agree with such precision. Using the calculated values of the inlet gradient and concentration from the backward integration of the differential equations the computation was reversed to determine if the same profile could be generated. The instability manifested itself again and curves 5, 6, 9 and 10 were generated on Figures 3 and 4.

Also shown on Figures 3 and 4 are curves 1 and 2 for plug flow with lumped constants. While the profiles differ the main difference lies in the maximum temperature attained at the hot spot and the fact that it takes longer to produce the same conversion in a diffusion reactor than it does in a plug flow reactor.

The calculations in this paper were performed for a typical turbulent flow case and the results on Figures 3 and 4 show the effect of the turbulent diffusivity. It has been pointed out (ref. (4)) that the Taylor diffusion coefficient is very sensitive to profile and hence it is possible that the temperature level in the reactor is sensitive to those parameters which affect the profile. Some additional calculations were made to determine the sensitivity of the backward integration of the differential equations to the assumed value at $v = 600$. A change of 1.4% in the concentration at $v = 600$ produced a change of 15% in the initial values at $v = 0$. These profiles are shown in Figure 5.

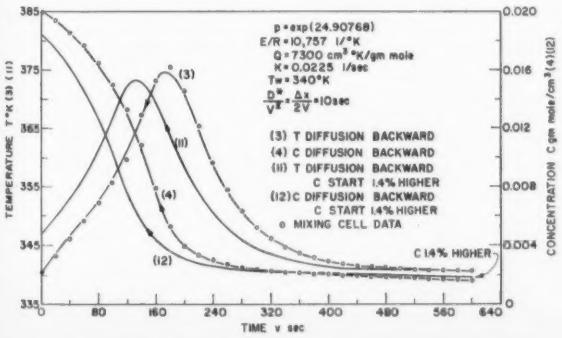
p = exp(24.90768)
E/R = 10,757 1/°K
Q = 7300 cm³ °K/gm mole
K = 0.0225 1/sec
Tw = 340°K
D*/V² = Δx/2V = 10 sec
(3) T DIFFUSION BACKWARD
(4) C DIFFUSION BACKWARD
(11) T DIFFUSION BACKWARD
C START 1.4% HIGHER
(12) C DIFFUSION BACKWARD
C START 1.4% HIGHER
o MIXING CELL DATA
C 14% HIGHER
TEMPERATURE T °K (3) (11)
CONCENTRATION C gm mole/cm³ (4)(12)
TIME v sec

Figure 5—Sensitivity of the backward integration. Profiles with respect to the starting value at $v = 600$.

Conclusions

It is assumed in this paper that the model of Taylor diffusion may be used in a tubular reactor in which there is chemical reaction and heat transfer. If the assumption is valid then it can be concluded that there are some effects, mainly in the reduction of the maximum temperature at the hot spot and increased length for the same conversion. These effects are not unexpected. A secondary conclusion is that a cell mixing model may be defined which gives profiles in very good agreement with the Taylor diffusion model for the reactor. It was also shown that if diffusion is coupled with exothermic chemical reaction the equations describing the process may become very unstable and the cell model may provide a reasonable method for the numerical solution. It is rather interesting that while a particular value of the cell size allows for axial diffusion (without back diffusion) a small value of Δx produces the lumped constant tubular solution. Hence a single mathematical model solves both problems.

Nomenclature

A = cross sectional area of tubular reactor
a = radius of tubular reactor
c = molar concentration
c_p = heat capacity
D = molecular diffusivity
D^* = effective Taylor diffusivity
E = activation energy for chemical reaction
h = overall heat transfer coefficient at tube wall
$K = \dfrac{hP}{Ac_p} = \dfrac{2h}{ac_p}$
n = cell number
p = frequency factor for reaction
$Q = -\dfrac{\Delta H}{c_p}$, heat of reaction parameter
T = reactor temperature
T_n = temperature in nth cell
T_w = ambient reactor temperature
v = x/V, residence time
V = average fluid velocity
x = reactor length variable

References

(1) Taylor, G. I., Proc. Roy. Soc. (London), **A219,** 186 (1953).
(2) Taylor, G. I., Proc. Roy. Soc. (London), **A220,** 446 (1954).
(3) Sjenitzer, F., Chem. Eng. Sci., **8,** 58 (1958).
(4) Tichacek, L. J., Barkelew, C. H., and Baron, T., A.I.Ch.E. Journal, **3,** 439 (1957).
(5) Fox, L., Numercial Solution of Two-Point Boundary Problem in Ordinary Differential Equations. Oxford University Press (1957).

★ ★ ★

Mass Transfer With and Without Chemical Reaction[1]

J. MARANGOZIS[2] and A. I. JOHNSON[2]

Rates of dissolution of cast solids in a baffled agitated vessel were obtained for the systems: Benzoic acid-water, o-salicylic acid-water, benzoic acid-22.5% acqueous glycerol and benzoic acid-41% aqueous glycerol. A new continuous technique was developed for the measurements, and the data were empirically correlated by the method of least squares with the equation

$$\frac{k_L^\circ l}{D} = 0.402 \left(\frac{\mu}{\rho D}\right)^{1/3} \left(\frac{rd^2\rho}{\mu}\right)^{0.65}$$

with a mean deviation of ± 5.8%.

The present data agreed qualitatively with the predictions of the turbulent boundary layer theory.

Reaction factors, k_L/k_L°, were also measured in the agitated vessels for the systems: Benzoic acid-aqueous sodium hydroxide solutions, benzoic acid-aqueous potassium hydroxide solutions, and o-salicylic acid-aqueous sodium hydroxide solutions. The data were found to depend strongly on the ratio of the reactant concentrations, C_B/C_{Ai}, in a manner quantitatively predicted by the boundary layer theory corrected for ion-diffusion effects.

Reaction factors were also measured in diaphragm-type diffusion cells for the system benzoic acid-sodium hydroxide. The results provided quantitative support for the ion-diffusion theory in a stagnant film.

There are numerous examples of processes involving diffusion accompanied by a chemical reaction.

Theoretically, at least, the subject has been treated in the literature almost exhaustively and as far as its mathematical complexities would allow. However, there are relatively fewer works reported which endeavored to investigate the problem experimentally.

In the present work, the problem of a rapid, heterogeneous chemical reaction was studied experimentally to gain an understanding of the rates and the mechanism involved in two different apparatus: a baffled agitated vessel operating under fully-developed turbulent conditions, and a diaphragm-type diffusion cell with the reaction occurring in the sintered disc under truly stagnant conditions.

[1]*Manuscript received March 1; accepted April 29, 1961.*
[2]*Department of Chemical Engineering, University of Toronto, Toronto, Ont. Contribution from the Department of Chemical Engineering, University of Toronto, Toronto, Ont. Dr. Johnson is now with the Department of Chemical Engineering, McMaster University, Hamilton, Ont.*

Historical Background

The Diffusion Layer Theory

In 1904 Nernst[1] advanced the concept of a saturated diffusion layer at a solid-liquid interface during the dissolution process. He suggested that the mass transfer coefficient, k_L°, be defined as

$$k_L^\circ = \frac{D}{x_L} \quad \ldots\ldots(1)$$

Whitman[2], and Lewis and Whitman[3] extended the diffusion layer concept to cover two films at a gas-liquid interface. The "two-film theory" was applied by Hatta[4,5] to the absorption of CO_2 in OH^- solutions. Figure 1 shows the concentration gradients according to Hatta for the general, rapid chemical reaction

$$A + B \rightarrow AB \quad \ldots\ldots(2)$$

Sherwood and Pigford[6] derived an equation for the mass transfer coefficient, k_L, namely,

$$k_L = \left(\frac{D_A}{x_L}\right)\left(1 + \frac{D_B}{D_A}\frac{C_B}{C_{Ai}}\right) \quad \ldots\ldots(3)$$

It has been reported[7,8,9] that solubilities, C_{Ai}, and diffusivities, D_A and D_B, of electrolytes are influenced by the presence of other ions. Therefore, in interpreting the rates according to theoretical models care should be exercised to include the aforementioned effects.

In 1931 Roller[10,11] demonstrated that the postulation of a stationary liquid film, at solid-liquid interfaces, was unrealistic. In accordance, other theoretical models ought to be developed.

The Penetration and Surface-Renewal Theories

In 1935 Higbie[12] advanced the "penetration model" of mass transfer by unsteady-state diffusion. He derived an equation for k_L° which was radically different from Equation (1),

$$k_L^\circ = 2\left(\frac{D}{\pi\theta}\right)^{1/2} \quad \ldots\ldots(4)$$

Danckwerts[13] and Sherwood and Pigford[6] derived an expression for the reaction factor, k_L/k_L°, for a rapid, bimolecular chemical reaction, namely

$$\frac{k_L}{k_L^\circ} = \frac{1}{erf\,(\alpha/D_A)^{1/2}} \quad \ldots\ldots(5)$$

where α is an integration constant which is a function of C_B/C_{Ai}, D_A and D_B.

Danckwerts[13] postulated a "surface-renewal" mechanism in which the surface is continually replaced at a constant rate, s, and transfer takes place by unsteady-state diffusion. He derived an equation identical to Equation (5) for this case, too. Hanratty[14] extended mathematically the Higbie and

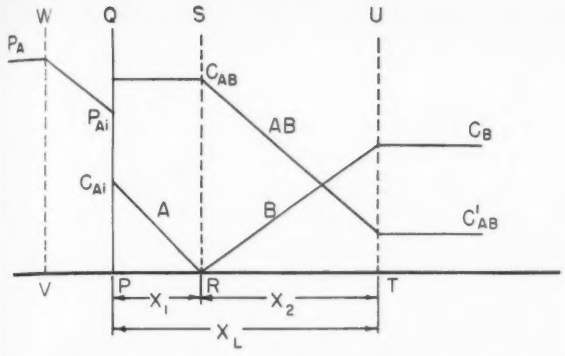

Figure 1—Sketch of concentration gradients according to Hatta theory of gas absorption with rapid chemical reaction in the liquid phase.

Danckwerts models, and compared his predictions with the experimental data of Lin, Moulton and Putnam[15].

The Development of the Boundary Layer Theory

According to Prandtl[16], for turbulent flows in pipes the fluid is thought to be divided into three layers: the laminar sublayer near the wall; the buffer region next to that; and the fully-turbulent core. Von Karman[17] obtained equations relating u^+ to y^+. In turbulent liquid streams, however, Lin, Moulton and Putnam[15] assumed that there is some eddy motion in the sublayer which decreases rapidly to zero at the wall. The analogy then of mass and momentum transfer leads to the equation

$$\frac{k_L^\circ}{\bar{u}}\phi_D = f/2 \qquad (6)$$

where $\bar{u}$ is the mean fluid velocity, f is the skin friction factor and ϕ_D is a complex function of the Schmidt number[15].

Sherwood and Ryan[18] used Deissler's analogy[19] to derive the following equations for k_L° and k_L/k_L° for a rapid reaction

$$\frac{\bar{u}}{k_L^\circ}\left(\frac{f}{2}\right)^{1/2} = \int_o^{y^+}\frac{dy^+}{1/Sc + \epsilon/\nu} = \phi(y^+, Sc) \qquad (7)$$

and

$$\frac{k_L}{k_L^\circ} = \frac{C_B}{C_{Ai}}\frac{\phi(y_o^+, Sc_A)}{[\phi(y_o^+, Sc_B) - \phi(y_R^+, Sc_B)]} \qquad (8)$$

where

$$y^+ = \frac{y}{\nu}\left(\frac{\tau_w}{\rho}\right)^{1/2} \qquad (9)$$

In the special case of $y_R^+ < 1$, Equation (8) was found[18] to reduce to the simple form

$$\frac{k_L}{k_L^\circ} \approx \left(\frac{Sc_B}{Sc_A}\right)^{1/3} + \left(\frac{Sc_A}{Sc_B}\right)^{2/3}\frac{C_B}{C_{Ai}} \qquad (10)$$

It is to be noted that Equation (10) was also derived by Potter[20], and by Friedlander and Litt[21] for *laminar* boundary flows.

Ion Diffusion in Interphase Mass Transfer

Vinograd and McBain[7] worked out the theory for the diffusion of ions in mixtures of electrolytes. The theoretical rate equations were found to agree satisfactorily with experiments of diffusion of ions with, through or against other ions[7,8]. Sherwood and Wei[22] combined Equation (3) with the principles of the Vinograd-McBain theory[7] to obtain the rate of mass transfer in the presence of ionic effects. A test of these calculations with experimental data is made in this paper. The significance of ion diffusion in boundary layer calculations is also demonstrated.

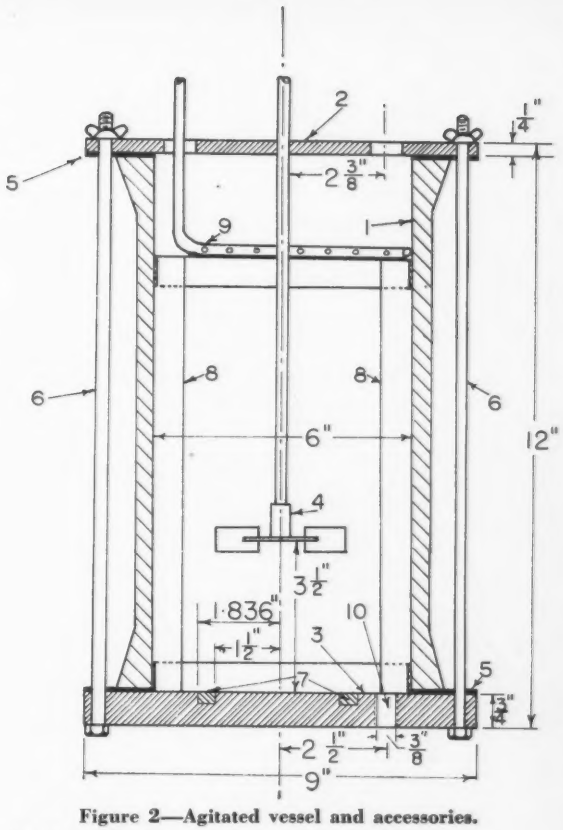

Figure 2—Agitated vessel and accessories.

1. glass cylinder
2. brass plate
3. stainless steel plate
4. impeller
5. gasket
6. tie rods
7. cast solid
8. baffle
9. liquid distributor
10. weir hole

Experimental Part

(a) Mass transfer in the agitated vessel.

The apparatus developed by Johnson and Huang[23] was used. It consisted of an agitated vessel the glass cylinder of which (6-in. I.D. and 12-in. high) was tightened between two plates as shown in Figure 2. A continuous operation was adopted mainly because constant conditions would prevail at steady state. Also, the calculations were simpler, easier and probably more reliable than if an unsteady-state operation had been adopted.

A shortcoming of the continuous technique was the difficulty encountered in the establishment of steady state as discussed below.

The bottom plate of the agitated vessel was of type 304 stainless steel in which a ¼-in.-deep circular ring depression was made. An organic acid was cast in the ring by the method described by Johnson and Huang[23]. The surface area of the cast material was 22.8 cm.^{2} The impeller was a 3-in.-diameter flat blade turbine with six blades made of stainless steel. It was driven by a Zero-Max variable motor, model M14, type G115-CCW. The speed of rotation was checked with a Strobotac and it was found to remain constant within less than ±1% of the set value over a four-hour period. Four vertical baffles mounted on two stainless steel rings were used as shown in Figure 2. A ⅜-in.-O.D., 7-in.-long stainless steel tube was bolted on the bottom plate to serve as an overflow weir.

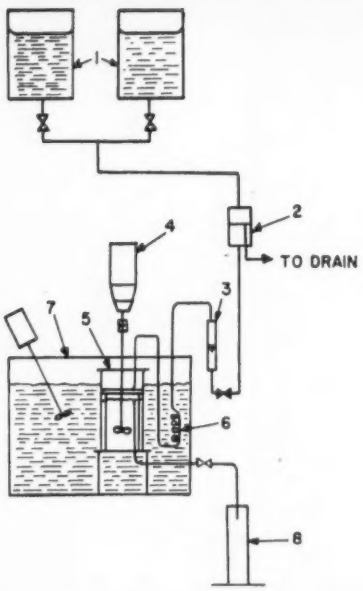

Figure 3—Schematic diagram of mass-transfer apparatus.

1. solvent reservoirs	**5. agitated vessel**
2. constant-head vessel	**6. solvent-heating coil**
3. solvent flow meter	**7. thermostated bath**
4. zero-max motor	**8. volumetric cylinder**

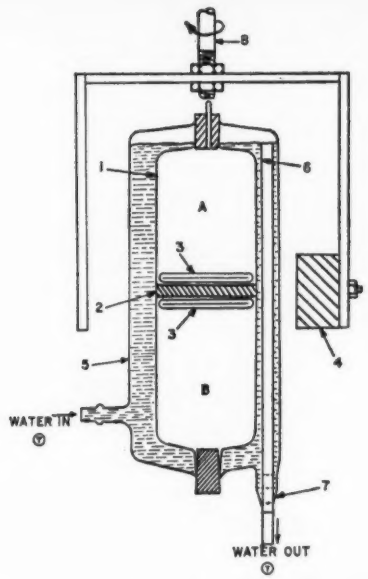

Figure 4—Schematic diagram of diaphragm diffusion cell.

1. diffusion cell	**5. jacket**
2. diaphragm	**6. overflow tube**
3. stirrer	**7. rubber joint**
4. magnet	**8. rotating shaft**

(T)—Temperature measurement.

A ¼-in.-O.D. stainless steel tube, shaped in the form of a ring, sitting on the top frame of the baffles, was employed to distribute the liquid fed into the tank through several small holes staggered along the circumference of the tube.

The agitated vessel was placed in a constant temperature bath held at 25 ± 0.1°C. during an experiment. A schematic diagram of the assembled mass transfer apparatus is shown in Figure 3. The systems investigated were: Benzoic acid-water, o-salicylic acid-water, benzoic acid-22.5% aqueous glycerol, benzoic acid-41% aqueous glycerol, benzoic acid-aqueous sodium hydroxide solutions, benzoic acid-aqueous potassium hydroxide solutions, and o-salicylic acid-aqueous sodium hydroxide solutions.

Three liters of solvent were brought to 25°C. and added to the tank to a level of 7-in. It was soon found that steady-state concentrations would be reached only after a considerable length of time had elapsed, which was too long to have a smooth surface maintained throughout. To overcome this difficulty, the solvent added to the tank in the case of the physical dissolution experiments was a solution of the organic acid at approximately the anticipated steady-state concentration. For the chemical dissolution experiments, the solvent added initially was a solution of caustic at about the anticipated concentration. Considerable trial and error effort was devoted to establishing the steady-state value; this should be considered as a shortcoming of the continuous operation method.

During a run, solvent from the reservoirs, 1, flowed through the constant head vessel, 2, the flowmeter, 3, the temperature-adjusting coil, 6, into the tank, 5, being uniformly distributed by the liquid distributor and running slowly along the wall of the tank. Samples of the effluent liquid were taken regularly for analysis by titration. The duration of a run was generally 90 minutes; longer runs were unreliable due to surface irregularities developed. Dissolution was allowed to proceed to the extent of 1 mm. in depth, only if a smooth, uniform surface was maintained. If the cast acid showed a rough surface at the end of a run, the results were discarded. These specifications restricted the use of caustic solutions to concentrations below 0.13 N., which corresponded to a value of the reaction factor of about 14 as will be discussed later.

Viscosities and densities of the glycerol solutions were measured according to standard methods. Diffusivities of the reactants in solutions of the reaction product were determined with diaphragm-type diffusion cells and were reported elsewhere[24]. A typical diffusion cell used in the diffusivity measurements is shown in Figure 4.

(b) Reaction factors in diaphragm cells.

A new procedure was adopted in this work for the measurement of reaction factors in diaphragm cells. Essentially, the diffusion cell illustrated in Figure 4 was equipped with a system for the continuous circulation of benzoic acid solution as shown in Figure 5. The solution was pumped from reservoir 1, by the stainless-steel, diaphragm pump 2, at a rate of about 10 cc./min. The constant-head vessel 3, was used to regulate the flow into the diffusion cell 4, at a rate of about 8 cc./min. by letting in a continuous stream of solution to maintain a constant acid concentration in the top compartment. The cell was magnetically stirred as shown and thermostated at 25 ± 0.1°C.

Sodium hydroxide solutions were contained in the bottom compartment and the reaction was allowed to proceed until 20 ~ 25% of the base had been neutralized. A preliminary diffusion of about two hours was allowed in order to establish a steady-state gradient in the pores of the diaphragm which was of "Fine" porosity, obtainable from Corning Glass, N.Y., U.S.A. After the preliminary diffusion, the solutions in the compartments were carefully replaced by fresh solutions and an ordinary run was started which usually lasted for one or two days. At the end of the experiment the concentrations of the solutions in the two compartments were determined by titration and reaction factors were calculated from the results.

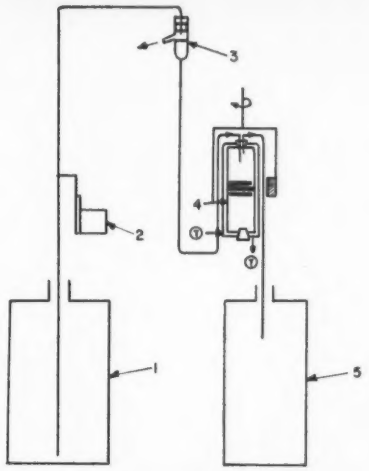

Figure 5—Schematic diagram of apparatus for reaction in diaphragm cells.

1. solution reservoir
2. diaphragm pump
3. constant-head vessel
4. diaphragm cell
5. overflow receptacle

(T)—Temperature measurement.

Discussion of Results

(a) **Physical mass transfer coefficient in the agitated vessel.**

Experimental and calculated results were listed in Table 1*. Mass transfer coefficients were plotted vs. the stirrer Reynolds number in Figure 6. For the first three systems the data showed that the mass transfer coefficient, $k_L°$, is proportional to approximately the $\frac{2}{3}$ power of Re up to a Reynolds number of 60,000. Beyond that value, the data for the first two systems show what appears to be a transition to a different variation of $k_L°$ with Re in the range $75{,}000 \leqslant Re \leqslant 110{,}000$.

In the more viscous solutions, it was not possible to reach this range of high Reynolds numbers with the present apparatus to study the phenomenon further. However, despite the reproducibility of the results in that region the authors have certain doubts as to the true significance of those results. It was visually observed that at high turbulence the liquid in the tank contained a substantial number of finely dispersed air bubbles. It was probable that air entrapped in the liquid might cause a reduction of the dissolution rate, for example, by reducing the convective effects of turbulence.

The data for the high Sc number system, benzoic acid-41% aqueous glycerol, showed a more complicated dependence of $k_L°$ on Re. This fact pointed to the conclusion that the relation among $k_L°$, Re and Sc groups may not be a simple one over a wide range of the variables. For a comparison of the present data with other investigations on solid-liquid mass transfer in agitated vessels the reader is referred elsewhere[24,25]. It would be extremely desirable to compare the present data directly with the predictions of the turbulent boundary layer Equations (6) or (7) previously discussed. Unfortunately, there are no data available in the literature for skin friction factors, f, in fully-baffled agitated vessels. Therefore, the best that can be done at the present is to correlate the data empirically and make qualitative comparisons with the theories.

The Gilliland-Sherwood form of correlation provides, on dimensional analysis basis, a satisfactory representation of mass

*Tables 1, 2 and 3 of this paper have been deposited as Document No. 6718 with the ADI Auxiliary Publications Project, Photoduplication Service, Library of Congress, Washington 25, D.C. A copy may be obtained by citing the Document No. and by remitting $5.00 for photoprints, or $2.25 for 35 mm. microfilm. Advance payment is required. Make cheques or money orders payable to: Chief, Photoduplication Service, Library of Congress.

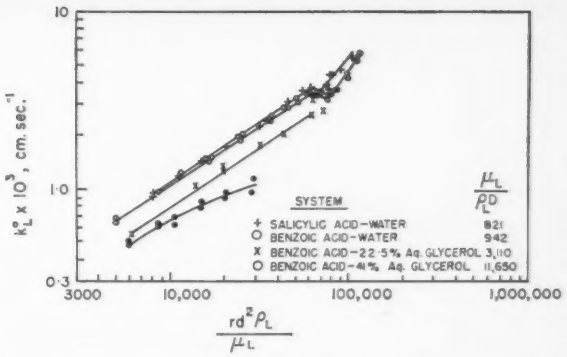

Figure 6—Mass transfer coefficient in agitated vessel vs. Reynolds number at 25°C.

transfer data for engineering purposes. The general form of this correlation is

$$Sh = a(Sc)^b (Re)^c \quad \ldots\ldots(11)$$

where a, b and c are constants to be determined from the data and the definition of the dimensionless groups is as follows:

$$Sh = \frac{k_L° l}{D};\ Sc = \frac{\mu_L}{\rho_L D};\ Re = \frac{rd^2\rho_L}{\mu_L}$$

where l = vessel diameter; d = rotor diameter; r = revolutions per second.

The present data were correlated with b taken as 0.25, 0.30, 0.333, 0.356, 0.42 and 0.50 respectively. The data up to Re = 60,000 only were considered.

The exponents 0.25, 0.42 and 0.50 showed a wide scattering of the results which indicated that these exponents were unsuitable for the correlation. A much better representation was obtained with the values 0.30, 0.333 and 0.356. The equation of the best straight line was obtained by the method of least squares in these three cases. The mean deviation of Sh number for the data is given below:

Equation	Mean Deviation of Sh
$(Sh) = 0.651\,(Sc)^{0.30}\,(Re)^{0.63}$	$\pm 6.1\%$ ..... (12)
$(Sh) = 0.402\,(Sc)^{0.333}\,(Re)^{0.65}$	$\pm 5.8\%$ ..... (13)
$(Sh) = 0.309\,(Sc)^{0.356}\,(Re)^{0.66}$	$\pm 6.7\%$ ..... (14)

Thus, the exponent b = 0.333 was thought to be the most suitable one to correlate the present data with the minimum scattering.

As shown by Potter[20] and Friedlander and Litt[21] in the case of *laminar* boundary layer flows on a flat plate, theoretical considerations predict the Sherwood number for mass transfer to be given in the form

$$(Sh) = 0.332\,(Sc)^{1/3}\,(Re)_x^{1/2} \quad \ldots\ldots(15)$$

A comparison of the empirical Equation (13) with the theoretically derived Equation (15) of the laminar boundary layer theory, suggests that the two disagreed on the effect of the Re number on mass transfer rates, which in turn indicates that the *laminar* boundary layer concept may not be true in the case of a fully baffled agitated vessel; this probably should be expected. An inquiry could be then made into the predictions of the *turbulent* boundary layer theory as discussed elsewhere in terms of Equation (7), namely,

$$\frac{k_L°}{\bar{u}}\,\phi(y^+, Sc) = \sqrt{f/2} \quad \ldots\ldots(7)$$

Based on a chart presented by Sherwood and Ryan[19] for the evaluation of $\phi(y^+, Sc)$ as a function of Sc up to y^+ = 200, it may be shown that in the range $1000 \leqslant Sc \leqslant 10{,}000$

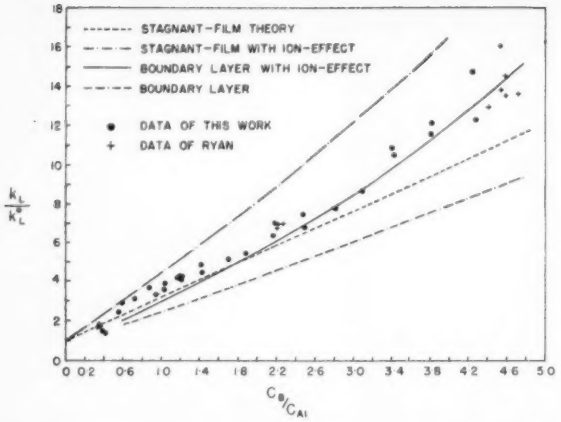

Figure 7 — Reaction factor data compared with theories benzoic acid-*NaOH* at 25°C.

$$\phi(200, Sc) \sim Sc^{2/3} \quad \ldots\ldots(16)$$

Hence, Equation (7) may be written in the form

$$k_L^\circ (Sc)^{2/3} \sim -\sqrt{f/2} \quad \ldots\ldots(17)$$

Multiplying through by l/D and rearranging

$$\frac{k_L^\circ l}{D} \sim \left(\frac{l}{d}\right)(Sc)^{1/3}(Re)_d \sqrt{f/2} \quad \ldots\ldots(18)$$

where l = vessel diameter, and d = stirrer diameter. If l/d is a constant, then Equation (18) could be written in a form similar to Equation (13), namely,

$$(Sh) = a(Sc)^{1/3}(Re)_d \sqrt{f/2} \quad \ldots\ldots(19)$$

where a is a numerical proportionality constant.

Again, regarding the Sc number effect the agreement between theory and experiment is striking. Unfortunately, the effects of the Reynolds number cannot be compared because there are no skin friction factor data available for a fully-baffled agitated vessel. However, from what is known[18] about f in fluid flow under turbulent conditions, a Re number effect such as demonstrated by the exponent 0.65 in Equation (13) may not be unlikely.

(b) Mass transfer with chemical reaction in the agitated vessel.

Rates of neutralization measured were tabulated in Table 2. Mass transfer coefficients, k_L, were calculated by taking into account changes in solubility of the acids due to the presence of the reaction product at the interface (see Figure 1). The corresponding k_L° values were obtained from Figure 6 and were corrected for any change in the physical properties of the systems by Equation (13). Diffusion coefficients of all reactants used were measured in solutions of the reaction products and reported elsewhere[24]. Reaction factors, k_L/k_L°, were tabulated in Table 2 and plotted in Figures 7, 9 and 11 for the three systems investigated here.

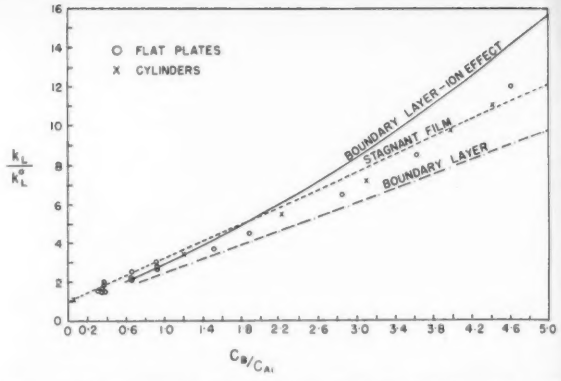

Figure 8—Reaction factors measured by Friedlander and Litt compared with theories: benzoic acid-*NaOH*, 25°C.

1. **System benzoic acid-sodium hydroxide.**

Results were plotted in Figure 7. Reproducibility of duplicate runs was on the average ± 6.6% and on the maximum ± 9%. The reaction factor tended to unity at low C_B/C_{Ai} values as would be expected. At high caustic concentrations ($C_B > 0.13N$) the dissolution rate was so fast that the surface area could not be maintained constant and wide scattering occurred. Data reported by Sherwood and Ryan[18] for dissolution of benzoic acid cylinders in sodium hydroxide solutions were plotted in Figure 7, too, for comparison with the present data. Very good agreement was observed between the two sets of data, notwithstanding the difference in the apparatus and techniques used.

The data were compared with the predictions of the theoretical models discussed previously. It may be noted that the stagnant-film theory line (Hatta[5]) was calculated by Equation (3), with the diffusivities D_B and D_A taken without ionic-effect considerations. This was taken care of in the top curve of Figure 7 which was calculated according to the ion-diffusion theory of Sherwood and Wei[22].

The bottom curve of Figure 7 was calculated by Equation (10) of the boundary layer theory, namely,

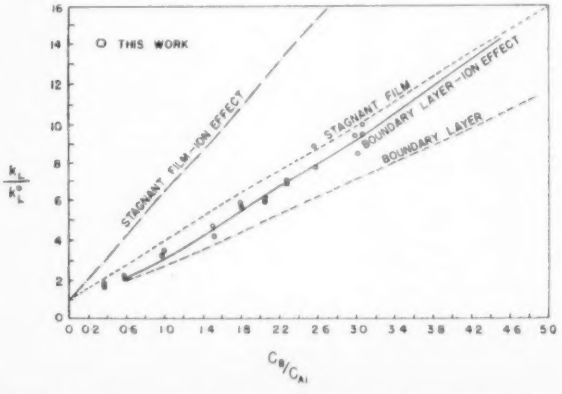

Figure 9—Comparison of reaction factor data with theories benzoic acid-*KOH*, 25°C.

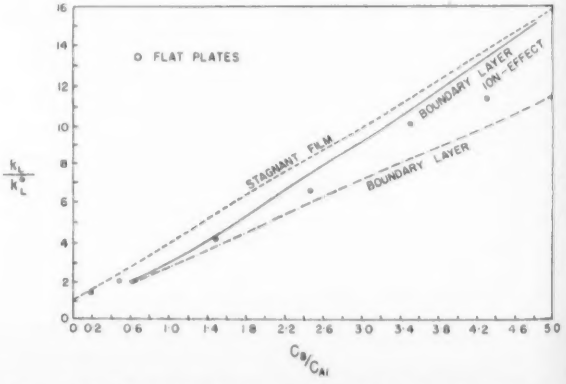

Figure 10—Reaction factors measured by Friedlander and Litt compared with theories benzoic acid-*KOH*, 25°C.

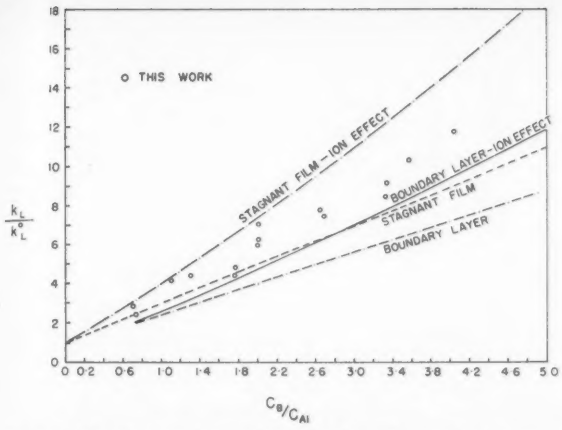

Figure 11—Comparison with theories of reaction factors for salicylic acid-*NaOH*, 25°C.

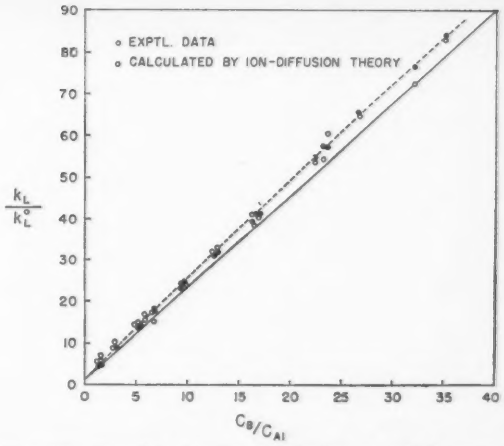

Figure 12—Reaction factors for diaphragm cell I compared with calculated values.

$$\frac{k_L}{k_L^\circ} \approx \left(\frac{Sc_B}{Sc_A}\right)^{1/3} + \left(\frac{Sc_A}{Sc_B}\right)^{2/3} \frac{C_B}{C_{Ai}} \quad \ldots\ldots\ldots\ldots (10)$$

The solid curve in Figure 7 was calculated by Equation (10), too, but allowance was made for the ionic effect on D_B and the viscosity effect on D_A from a calculation of the sodium benzoate concentrations at the interface and parallel diffusivity data.

In the region studied, the data appeared to be better represented by the solid curve (boundary layer theory with ionic effects on diffusivity) rather than by any other of the theoretical lines. It would be legitimate, therefore, to conclude that, in this particular case, the data give support to the mechanism suggested by the boundary layer theory, and that the experimental results justified the assumptions made in the derivation of Equation (10).

Litt and Friedlander[26] reported an experimental study of reaction factors measured for flat surfaces and cylinders of benzoic acid supported in a flow tunnel.

Their data were recalculated and plotted in Figure 8, along with the predictions of the theories which were slightly different from Figure 7, since the salt concentration C_{AB} was practically zero.

In the region $o < C_B/C_{Ai} < 1.5$, the data were in good agreement with the boundary layer theory corrected for ionic effects. At higher concentrations, however, the data seemed to be better represented by the stagnant-film line, which was calculated with no ionic effects taken into account. The data were rather limited in number, and reproducibility should be expected to be of the order of at least ± 10% in the higher concentration range. Litt and Friedlander operated their apparatus expecting to be in the laminar boundary layer flow region ($Re_x < 50{,}000$). As they concluded from their physical dissolution experiments, however, turbulence was induced in their apparatus reflecting in a substantial increase of the dissolution rate. The treatment of the reaction factor data by Litt and Friedlander[26] was rather oversimplified. They assumed that Sc_A and Sc_B remain constant over the whole range of C_B/C_{Ai} studied.

Actually, both Sc_A and Sc_B vary considerably with C_B/C_{Ai} if one considers ionic and viscosity effects. By the viscosity effect alone (because of the presence of benzoate at the interface), Sc_A attains a value of 1460 at $C_B/C_{Ai} = 5$, hence Sc_B is calculated to be 490 instead of 296 estimated by Litt and Friedlander[26]. For a further discussion of these data the reader is referred to Reference (24).

2. System benzoic acid-potassium hydroxide.

Data of this work listed in Table 2 were plotted in Figure 9 and compared with the theories. Reproducibility of duplicate runs was on the average ± 6.8% and on the maximum ± 13.5% at high C_B concentrations. The data were below the Hatta line in contrast to the data of Figure 7 which were above. The deviation of the data from the boundary layer theory line with ionic correction was, on the average, ± 3.8% with a maximum of ± 11%. Similar, but limited, data reported by Litt and Friedlander[26] were plotted in Figure 10. These data were considerably below the Hatta line, too, and they seemed to be about half way between the two boundary-layer theory lines.

3. System salicylic acid-sodium hydroxide.

Data of this work were listed in Table 2 and plotted in Figure 11. Reproducibility was on the average ± 8.9%. The lower precision was due to the smaller solubility of salicylic acid and hence to greater relative analytical errors. The data shown in Figure 11 do not agree with any of the theoretical models. The boundary layer theory line corrected for ionic effects was about 15% below the data and almost parallel to them. There are no other data reported in the literature for this system for comparison. Some data reported by Hsu[27] were considered as unreliable because of poor self-consistency possibly due to the unsteady-state method of measurement.

With regard to the data shown in Figure 11 there is still some doubt concerning the solubility data[24] of salicylic acid in sodium salicylate solutions whence C_{Ai} was obtained. These solubilities at 25°C. were calculated from activity coefficients obtained from data reported at 20.1°C.[9] and the solubility value in water taken as 0.0159M. at 25°C. Solubility measurements at 25°C. made in this work from super-saturated solutions of salicylic acid in sodium salicylate solutions agreed with the predicted values within 2 ~ 3%, but measurements made from under-saturated solutions were considerably lower.

(c) Reaction-factor measurements in diaphragm cells.

Certainly, in an agitated vessel with baffles the hydrodynamics is complicated and at the present not well understood. However, in a well stirred, diaphragm-type diffusion cell, there is unanimous agreement[7,8,22,28,29] that the process of diffusion takes place in a truly stagnant layer of liquid with no complicating convention effects.

In this work, reaction factors were measured in a diaphragm cell in an effort to test the validity of the stagnant-film, ion-diffusion theory. Experimental results obtained for the system benzoic acid-sodium hydroxide in two cells were listed in Table 3. The reaction factors were determined using Equation (20) the derivation of which is given in Reference (24),

$$\frac{k_L}{k_L^\circ} = \frac{\bar{J}_B(1/V_1 + 1/V_2)}{2.303\, D_A C_A K} \quad \ldots\ldots\ldots\ldots (20)$$

Calculated values of reaction factors were obtained from Equation (21) below

$$\frac{k_L}{k_L^\circ} = 1 + \frac{D_B}{D_A}\frac{C_B}{C_A} \quad \ldots\ldots\ldots\ldots\ldots\ldots (21)$$

where C_B is the arithmetic mean concentration of sodium hydroxide at the beginning and the end of the experiment.

The data were plotted in Figure 12, and compared with the calculated values. The concentrations of the reaction product in the diaphragm were estimated[24] and values of D_B and D_A were obtained from parallel diffusivity experiments. The calculated values were within ± 7.4% of the experimental results, while the Hatta line was about 11% below the data. It was concluded that there is favourable agreement with the stagnant-film, ion-diffusion theory of mass transfer.

Another important remark to be made is that, in these experiments, the "collision effect" between the counter-diffusing columns of OH^- and benzoate ions, if any, ought to be very small in this case. Perhaps, the effect of this phenomenon might be more evident at higher reaction product concentrations.

Conclusions

On the basis of the experimental data obtained in this investigation for mass transfer coefficients without chemical reaction for solid-liquid systems in baffled agitated vessels, it was established that the Sherwood number depends on the ⅓ power of the Schmidt number and the 0.65 power of the stirrer Reynolds number. The present data are about 10% lower than similar data reported by Johnson and Huang[23].

The exponent ⅓ on the *Sc* group is significant in that it is in good agreement with the prediction of the boundary layer theory of mass transfer. The exponent 0.65 on the *Re* group is in disagreement with the *laminar* boundary layer theory but it was thought to be in qualitative agreement with the *turbulent* boundary layer concept.

Reaction factors in agitated vessels measured for solid-liquid neutralization systems were found to depend strongly on the concentration ratio of the reactants, C_B/C_{Ai}, in a manner quantitatively predicted by the boundary layer theory corrected for ionic effects on the diffusivities of the reacting species. The data were in agreement with similar data from rotating dissolving cylinders, a fact which indicated that the geometry of the apparatus is insignificant.

Reaction factors in diaphragm-type diffusion cells were obtained and were found to quantitatively support the theory of ion diffusion in a stagnant film.

Acknowledgement

The receipt of a National Research Council Studentship by J. Marangozis in support of this work, is gratefully acknowledged.

Nomenclature

a,b,c	=	Constants
C	=	Concentration, g. moles cm.$^{-3}$ or g. equiv. cm.$^{-3}$
D	=	Diffusion coefficient, cm.^{2} sec.$^{-1}$
d	=	Stirrer diameter, cm.
E_D	=	Eddy diffusivity, cm.^{2} sec.$^{-1}$
f	=	Skin friction factor.
J	=	Solute mean flux, g. moles. cm.$^{-2}$ sec.$^{-1}$ or g. equiv. cm.$^{-2}$ sec.$^{-1}$
k_L	=	Mass transfer coefficient with chemical reaction, cm. sec.$^{-1}$
k_L°	=	Mass transfer coefficient without chemical reaction, cm. sec.$^{-1}$
K	=	Diffusion cell constant, cm.$^{-2}$
l	=	Agitated vessel diameter, cm.
N	=	Rate of mass transfer, g. moles. cm.$^{-2}$ sec.$^{-1}$ or g. equiv. cm.$^{-2}$ sec.$^{-1}$
r	=	Revolutions of stirrer per second.
$(Re)_d$	=	Stirrer Reynolds number, $rd^2\rho/\mu$
s	=	Rate of surface renewal, sec.$^{-1}$
Sc	=	Schmidt number, $\mu/\rho D$
Sh	=	Sherwood number, $k_L^\circ l/D$
St	=	Stanton number, $k_L^\circ/\bar{u}$
T	=	Temperature, °K.
$\bar{u}$	=	Mean fluid velocity, cm. sec.$^{-1}$
V_1, V_2	=	Volumes of compartments 1 and 2, cm.^{3}
x	=	Distance along diffusion path, cm.
x_L	=	Thickness of diffusion layer, cm.
y	=	Distance from wall, cm.
y^+	=	Dimensionless distance from wall defined by Eq. (9)

Greek Letters

α	=	Constant
ϵ	=	Eddy kinematic viscosity, cm.^{2} sec.$^{-1}$
θ	=	Time, sec.
μ	=	Fluid viscosity, poises or g. cm.$^{-1}$ sec.$^{-1}$
ν	=	Kinematic viscosity, μ/ρ, cm.^{2} sec.$^{-1}$
ρ	=	Fluid density, g. cm.$^{-3}$
τ_w	=	Shear stress at the wall, dyn. cm.$^{-2}$
$\phi(\ )$	=	Denotes function

Subscripts

A,B	=	Solutes A,B
D	=	Diffusion
i	=	Interface
L	=	Liquid
w	=	Wall

References

(1) Nernst, W., Z. Physik. Chem., **47,** 52 (1904).
(2) Whitman, W. G., Chem. & Met. Eng., **24,** 146 (1923).
(3) Lewis, W. K., and Whitman, W. G., Ind. Eng. Chem., **16,** 1215 (1924).
(4) Hatta, S., Tech. Repts. Tôhoku Imp. Univ., **8,** 1 (1928).
(5) Hatta, S., J. Soc. Chem. Ind. (Japan), **31,** 869 (1928).
(6) Sherwood, T. K., and Pigford, R. L., "Absorption and Extraction", McGraw-Hill Book Company, Inc., New York, 1952.
(7) Vinograd, J. R., and McBain, J. W., J. Am. Chem. Soc., **63,** 2008 (1941).
(8) Dean, R. B., J. Am. Chem. Soc., **67,** 31 (1945).
(9) Seidell, A., "Solubilities of Organic Compounds", 3rd Edition, Vol. II, D. Van Nostrand Co., Inc., New York, 1941.
(10) Roller, P. S., J. Phys. Chem., **35,** 1113 (1931).
(11) Roller, P. S., J. Phys. Chem., **36,** 1202 (1932).
(12) Higbie, R., Trans. Am. Inst. Chem. Engrs., **31,** 365 (1935).
(13) Danckwerts, P. V., Ind. Eng. Chem., **43,** 1460 (1951).
(14) Hanratty, T. J., A.I.Ch.E. Journal, **2,** 359 (1956).
(15) Lin, C. S., Moulton, R. W., and Putnam, C. L., Ind. Eng. Chem., **45,** 636 (1953); Ind. Eng. Chem., **45,** 640 (1953).
(16) Prandtl, L., Physik. Z., **29,** 487 (1928).
(17) Von Karman, T., Trans. Am. Soc. Mech. Engrs., **61,** 705 (1939).
(18) Sherwood, T. K., and Ryan, J. M., Chem. Eng. Sci., **11,** 81 (1959).
(19) Deissler, R. G., N.A.C.A. Report 1210, 1955.
(20) Potter, O. E., Trans. Inst. Chem. Engrs., **36,** 415 (1958).
(21) Friedlander, S. K., and Litt, M., Chem. Eng. Sci., **7,** 229 (1958).
(22) Sherwood, T. K., and Wei, J. C., A.I.Ch.E. Journal, **1,** 522 (1955).
(23) Johnson, A. I., and Huang, C.-J., A.I.Ch.E. Journal, **2,** 412 (1956).
(24) Marangozis, J., Ph.D. Thesis, Chem. Eng. Dept., Univ. Toronto, 1960.
(25) Marangozis, J., and Johnson, A. I., manuscript submitted for publication Can. J. Chem. Eng.
(26) Litt, M., and Friedlander, S. K., A.I.Ch.E. Journal, **5,** 483 (1959).
(27) Hsu, C.-J., M.S. Thesis, Chem. Eng. Dept., Univ. Houston, 1959.
(28) Robinson, R. A., and Stokes, R. H., "Electrolyte Solutions", Butterworth's Scientific Publications, 2nd Ed., London, 1959.
(29) Gordon, A. R., Ann. N.Y. Acad. Sci., **46,** 285 (1945).

★ ★ ★

High-Speed Photography in the Study of Two-Phase Flow[1]

R. A. S. BROWN[2] *and G. W. GOVIER*[3]

Some of the possible applications of high-speed motion picture photography in the study of two-phase, two-fluid flows are outlined. These include measurements of ripple or wave velocities in annular flow and bubble velocities in bubble and slug flows. Qualitatively, the motion pictures permit better understanding of the interactions between the two phases.

The equipment being used in the present photographic study of vertical flow of oil-water mixtures is described. A 16-mm. "Fastax" high-speed motion picture camera having speeds to 8000 frames/sec. is being used in these studies. Auxiliary equipment includes a high intensity light source and a timing pulse generator.

In the oil-water system being studied, bubble groups and bubble clusters are formed which rise at approximately constant velocities. Very little effect of bubble size on the velocity of the bubble was noted except in a few instances where the bubbles appeared to be close to the wall. Preliminary results of the effects of superficial oil and water velocities on the bubble velocity are presented.

Some other photographic techniques which might find application in the analysis of two-phase flows are discussed.

It has been apparent for some time that a need exists for a more fundamental approach to the analysis of the flow of two-phase mixtures. While numerous empirical correlations have been proposed within the last few years[1,2] no great improvement in the understanding or the accuracy of prediction of flow characteristics has resulted. There have, however, been a few notable attempts to approach the analysis of individual flow patterns from a fundamental basis[3,4,5]. Mechanistic analyses such as these are promising and should eventually be more productive than the strictly empirical approach — important though that approach is.

At the University of Alberta, high-speed motion pictures are being taken to serve as a guide in the analysis of the flow of two-phase systems. Motion picture photography is useful for this purpose since the interactions between phases can be observed directly and accurate measurements of the flow geometry and the phase velocities may be obtained. To date, most of the tests have been concerned with the vertical flow of oil-water mixtures in the bubble and slug flow regions.

In bubble flow, high-speed motion pictures can yield information on individual bubble and bubble cluster velocities and their paths of rise, distribution of bubble diameters, in situ volume ratio of the phases, interactions between bubbles and interactions between the phases. The latter would include oscillation of the bubbles if the frequency was sufficiently low to be observable.

High speed motion picture photography should be equally productive of useful information in the other flow regions. A survey of the measurable characteristics would include bubble velocity and shape in slug flow and ripple or wave velocity, amplitude and period in annular flow, as well as in situ volume ratios of the phases. In other regions, such as the froth flow region, so little is known about the flow that possible measurements can only be surmised until some tests are made. For some of these cases, also, special methods of lighting may be required to outline the flow structure.

The above measurements are some of those obtainable from the motion pictures. In all of these, the main purpose is to obtain the variation of the observed characteristics with the flow rates and the properties of the two phases and to learn from this more of the mechanisms important in the different regions.

The Bubble Flow Region—Theoretical Considerations

Consider a mixture of two phases — one continuous, the other dispersed as bubbles — entering a vertical section of tube in time t^*. Let the superficial velocity of the continuous (reference) phase be V_R and that of the dispersed (second) phase be V_S. The flow is in the bubble or slug flow region with N bubbles entering the section in the time t^* and having individual volumes v_i and instantaneous velocities V_{bi}. Assume that none of the bubbles introduced in the time interval overtake bubbles introduced before the time $t = 0$. At $t = t^*$, the bubbles will extend over some length L where

$$L = \int_0^{t^*} V_{bp}\,dt \qquad (1)$$

and bubble p has moved furthest up the tube. The volume of second phase which has entered is

$$\sum_0^N v_i = V_S A_t t^* \qquad (2)$$

and hence the volume of continuous phase is

$$LA_t - V_S A_t t^* = A_t \int_0^{t^*} V_{bp}\,dt - V_S A_t t^* \qquad (3)$$

[1]*Manuscript received January 17; accepted May 5, 1961.*
[2]*Ph.D. candidate, Department of Chemical and Petroleum Engineering, University of Alberta, Edmonton, Alta.*
[3]*Professor of Chemical Engineering, Dean of Faculty of Engineering, University of Alberta, Edmonton, Alta.*

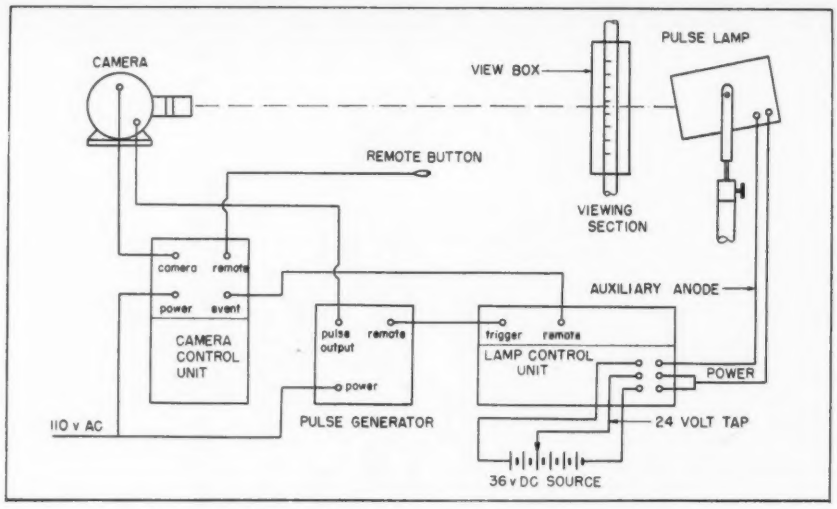

Figure 1—Schematic diagram of photographic equipment.

If t^* is sufficiently great, the volume ratio of second phase to reference phase will be characteristic of the flow and the holdup ratio (1) may be written

$$H_R = \frac{V_S/V_R}{A_t V_{St}^*/(A_t \int_0^{t^*} V_{bp} dt - A_t V_{St}^*)}$$

$$= \frac{\int_0^{t^*} V_{bp} dt - V_{St}^*}{V_{Rt}^*} \quad \ldots\ldots(4)$$

For the special case where all bubbles are moving with the same velocity, V_b, Equation (4) becomes

$$H_R = \frac{V_b - V_S}{V_R} \quad \ldots\ldots(5)$$

The average density of the mixture can be written as

$$\rho_a = \rho_S \frac{V_{St}^*}{\int_0^{t^*} V_{bp} dt} + \rho_R \frac{\int_0^{t^*} V_{bp} dt - V_{St}^*}{\int_0^{t^*} V_{bp} dt} \quad \ldots\ldots(6)$$

or, for constant bubble velocity

$$\rho_a = \rho_S \frac{V_S}{V_b} + \rho_R \frac{V_b - V_S}{V_b}$$

$$= \rho_R - (\rho_R - \rho_S) \frac{V_S}{V_b} \quad \ldots\ldots(7)$$

The pressure drop over a section of vertical tube is composed of a hydrostatic head component and a frictional component. For the bubble and slug flow regions, the hydrostatic component of the unit pressure drop is equal to the average density of the mixture in the tube and

$$\frac{\Delta P}{\Delta x} \approx \rho_a \quad \ldots\ldots(8)$$

In the bubble flow region, the frictional pressure drop should be very closely approximated by the pressure drop calculated for reference fluid flowing alone at the mixture velocity, Vm.

ie.
$$\frac{\Delta P}{\Delta x} = \rho_a + \frac{2f\rho_R V_m^2}{g_c D} \quad \ldots\ldots(9)$$

where
$$V_m = V_R + V_S$$

and f depends upon a Reynolds number calculated as

$$Re = \frac{D V_m \rho_R}{\mu_R}$$

The calculation for slug flow is the same in principle although some differences exist due to the restricted cross-section for flow of the reference phase.

Experimental Equipment

The experimental equipment is shown schematically in Figure 1 and photographs of the working level of the equipment well and of the control equipment are given in Figures 2 and 3. A description of the flow system being used for the present study of oil-water mixtures has been given previously[6]. The test section is a cellulose acetate butyrate tube having an inside diameter of 1.038-in. The flow tube is 37-ft. long and the

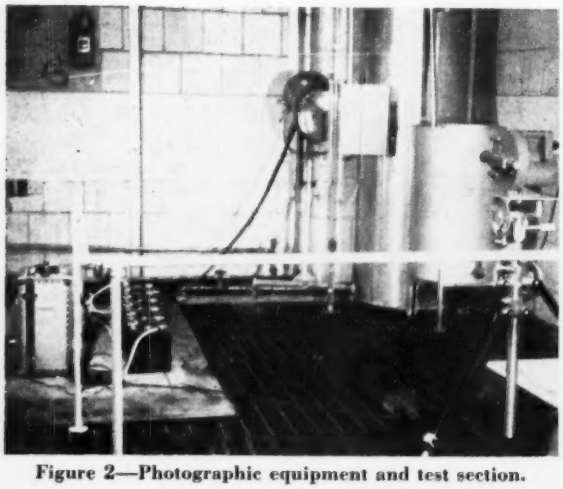

Figure 2—Photographic equipment and test section.

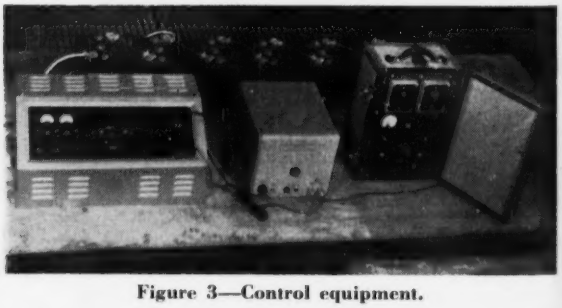

Figure 3—Control equipment.

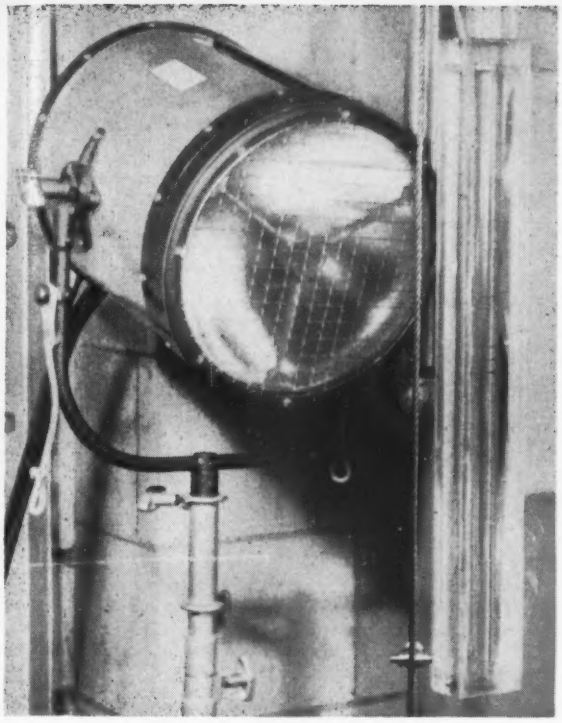

Figure 4—Viewing section.

viewing section is 23-ft. above the mixing tee. The test section for pressure drop is 28.37-ft. long and the lower tap is about 8-ft. above the mixing tee. Properties of the oil and water are given in Table 1.

The tube has been inscribed in the viewing section with lines ½, 1, 3 and 6-in. from a reference line. This section of tube is enclosed in a view-box shown in Figure 4 consisting of a two-foot length of 3-in. I.D. Lucite tube which has been cut lengthwise along a chord and faced with ⅛-in. Lucite sheet. End pieces are Lucite discs which were machined to fit over the flow tube and centre it in the view-box. A liquid seal around the flow tube is obtained with O-rings set in grooves in the end pieces. A drain hole with tap at the bottom of the view box and air holes at the top permit addition and removal of liquid around the flow tube.

Photographic equipment was purchased as a unit prepared by the Wollensak Optical Company and consists of camera, control or "Goose" unit, high intensity Xenon lamp unit and 100/1000 cycles per second timing pulse generator. The

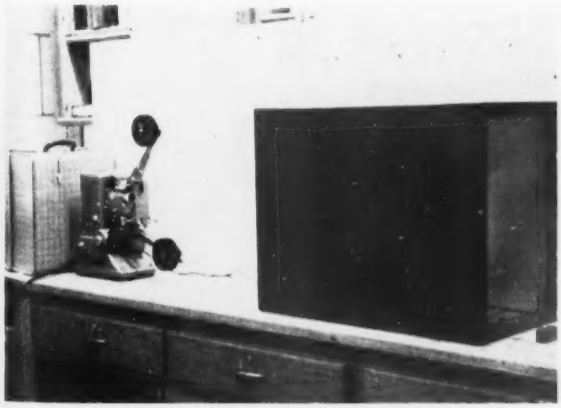

Figure 5—Projection equipment used in analysis.

TABLE 1

PHYSICAL PROPERTIES OF THE LIQUIDS

Water	
Density	62.3 lb./ft.³ at 72.0°F.
Viscosity	0.936 cp. at 72.0°F.
Oil (Marcol GX)	
Density	53.00 lb./ft.³ at 72.0°F.
Viscosity	20.09 cp. at 72.0°F.
Interfacial Tension	50.34 dynes/cm. at 77.0°F.

camera is a Fastax WF 3 model which uses 100-ft. reels of 16 mm. film. In this camera, which has a maximum repetition rate of about 8000 frames/sec., the image is stabilized on the continuously moving film by a prism which rotates in synchronism with the film motion. Different film speeds are obtained by adjusting the voltage applied to the universal motors of the camera and the repetition rate at any point is indicated by timing pulses registered on the film during operation. A prism arrangement permits through-the-lens focussing. The high intensity light source is a discharge lamp which can be pulsed at three power levels or used as a semi-continuous source at a fourth, lower, power level. Direct current for the lamp is supplied by a bank of six 6-volt automotive batteries having a fairly high current rating.

The pulse lamp was positioned directly behind the viewing section as shown in Figures 2 and 4 since preliminary tests indicated that better contrast could be obtained with back lighting. It was necessary to shield the camera from direct light from the lamp (which might cause fogging of the film) by installing light shields on each side of the view box.

Kodak Tri-X negative film (Type 7233) has been used for most of the tests presented here although some tests have been made with DuPont Superior 4 Negative Film (Type 928A). The processing is quite simple for either of these films.

The film was analyzed by projecting it on a small rear-projection screen as shown in Figure 5. The projector used was a Wollensak Motion Analysis machine which permits single frame projection, has fairly good registration and is equipped with a frame counter. The measurements of the flow geometry and velocities were aided by superimposing a grid on the projected image. This grid was a photographic copy on Mylar film of a sheet of standard arithmetic graph paper (10 × 10 to the ½-in.) and was placed directly against the rear projection screen.

Experimental Procedure

For a given position of the camera with respect to the viewing section, the combination of lens and extension tube used was determined by the field of view desired which, in this case, was the length of viewing section to be observed. This was dependent, in turn, on the information desired from the film. If the viewing length is long, an individual flow configuration can be observed to determine the changes in its behavior with time (or position) and its average velocity. Shorter viewing lengths (greater magnification) are better suited to the determination of geometrical characteristics of individual configurations and instantaneous velocities.

The next factor to be considered was the picture repetition rate desired. A lower limit on the repetition rate is set by the velocity of the pattern being observed and the resolution of the optical system being used. Stated simply, if the subject moves a distance greater than the resolution limit of the optical system during the period of exposure the image will appear blurred. (A good discussion on the requirements for "stopping" motion by high speed motion picture photography is given by Hyzer[7].) The choice of film speed is also determined, therefore, by the purpose of the test. If the study is directed towards a study of bubble vibration or oscillation rather than towards the deter-

TABLE 2
EXPERIMENTAL CONDITIONS

Test No.	Water Rate		Oil Rate		Pressure Drop ft. H_2O/ft.	Holdup Ratio H_R
	ft.³/sec.	ft./sec.[a]	ft.³/sec.	ft./sec.[a]		
18	0.00586	1.0	0.00127	0.2165	0.990[b]	1.45[b]
19	0.00586	1.0	0.000434	0.0739	1.002	1.73
26	0.00586	1.0	0.000339	0.0577	1.00[b]	1.67[b]
27	0.00188	0.32	0.000434	0.0739	0.990	2.20
28	0.0106	1.8	0.000434	0.0739	1.014	1.52
29	0.00586	1.0	0.000902	0.154	0.998[b]	1.50[b]
31	0.00586	1.0	0.00507	0.865	0.960	1.44
34	0.00586	1.0	0.00264	0.449	0.975[b]	1.42[b]
35	0.00586	1.0	0.00507	0.865	0.960	1.44

[a]Superficial lineal velocity
[b]Interpolated from Reference (9)

TABLE 3
PHOTOGRAPHIC CONDITIONS

Test No.	Distance Camera to Tube	Lens	Lighting[a]	Nominal Repetition Rate	Lens Aperature f
18	8 ft. 2 in.	153.6 mm.	2.5 kw pulse	1500	32
19	8 ft. 2 in.	153.6 mm.	2.5 kw pulse	1500	32
26	29 3/8 in.	50 mm.	Simmer	1500	11
27	29 3/8 in.	50 mm.	Simmer	1500	11
28	29 3/8 in.	50 mm.	Simmer	1500	5.6
29	29 3/8 in.	50 mm.	Simmer	1500	5.6
31	8 ft. 2 in.	153.6 mm.	Simmer	1500	6.5
34	8 ft. 2 in.	153.6 mm.	Simmer	1500	6
35	8 ft. 2 in.	153.6 mm.	Simmer	1500	6.5

[a]Pulse lamp 1 foot behind and slightly above viewing section.

mination of average bubble velocities, higher repetition rates will be required because of the greater velocity of the observed phenomenon.

Knowing the repetition rate, the lens setting for a given lighting arrangement may be determined. Some difficulty was experienced with the choice of lens settings for the back lighting arrangements used because the incident light meter gave settings which were too low. Experience should indicate, however, the correction which must be applied to the meter reading.

Experimental flow conditions for the tests reported here are given in Table 2, while the photographic conditions are noted in Table 3. As the main interest in these tests was in average velocities of bubbles and bubble groups, a relatively low repetition rate was used.

Experimental Results

The lighting method used gave fairly good contrast and the bubble motion is easily observable. The bubble image is rather hazy and the reason for this has not yet been determined. This lack of definition does not appear serious except in the size determination of small bubbles where the percentage error may be large. Velocity measurements are quite simply made and there appears to be very little possibility of judgment errors in the determination.

These initial investigations with high-speed motion picture techniques have been made in the bubble and slug flow regions for a system consisting of a white oil and water. The set of tests comprising the present investigation includes six tests at the same oil velocity and varying water velocity and an additional two tests at one of the water velocities and different oil velocities. One check run was also obtained at a high oil flow rate. The water and oil flow rates are given in Table 2 along with the pressure drop and hold-up values for the test conditions as obtained from earlier results[6].

The most notable flow characteristic obtained from the films was the relative constancy of the velocity of rise of bubble groups. The size of the individual bubble has no observable effect on its velocity of rise when in a bubble group. This effect, which might be expected when the bubbles are clustered together would not necessarily be expected for more open groupings of bubbles where the individual bubbles might be expected to rise in relation to their sizes. The result indicates that it may be more appropriate in some cases to treat bubble flow as a type of slug flow rather than as a modified single bubble flow.

Figure 6 shows the change in bubble size and grouping for superficial water velocities of 0.32, 1.0 and 1.8-ft./sec. with a superficial oil velocity of 0.0739-ft./sec. Similarly, the flow patterns for six superficial velocities at a superficial water velocity of 1.0-ft./sec. are shown in Figure 7. In each case the leading end of a group of bubbles is shown. Figure 7 indicates the development of slug flow as the flow rate of the second phase (oil) is increased at a constant flow rate of reference phase (water). The highest oil flow rate is well within the slug flow region and approaching froth flow. The transition between regimes I and II occurs at a superficial oil velocity of about 1.25-ft./sec.

The bubble velocities obtained in the present investigation are given in Column 2 of Table 4. Columns 3 and 4 show the comparison between the holdup ratio obtained directly[8] and that calculated from the bubble velocity with Equation(5). The average density of the mixture in the tube, obtained from Equation (7), is given in column 5 while columns 6 and 7 show the comparison between the experimental pressure drop and that calculated from Equation (9).

Figure 8 indicates the effect of superficial water velocity on the bubble velocity for a superficial oil velocity of 0.0739-ft./sec. The dashed line indicates the mixture velocity. The slip velocity, defined as the difference between the bubble velocity and the mixture velocity, increases from 0.39-ft./sec. at a mixture

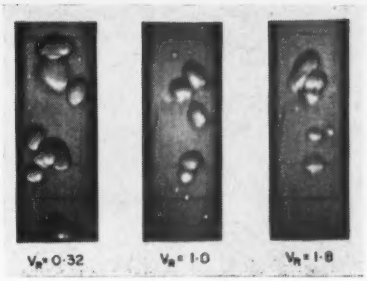

Figure 6—Flow patterns for a superficial oil velocity, V_s, of 0.0739-ft./sec.

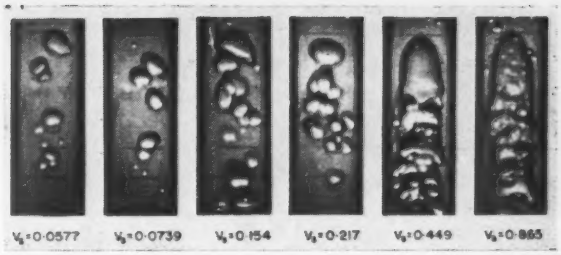

Figure 7—Flow patterns for a superficial water velocity, V_s, of 1.0-ft./sec.

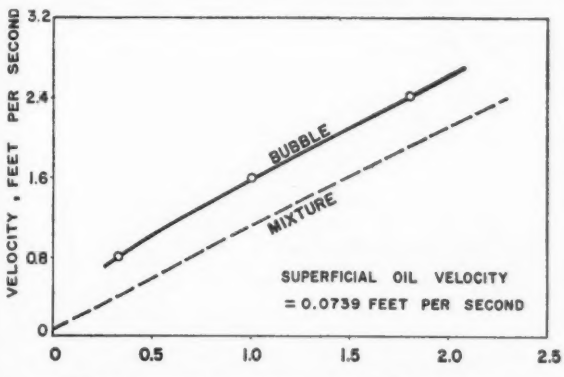

Figure 8—Effect of water velocity on bubble velocity.

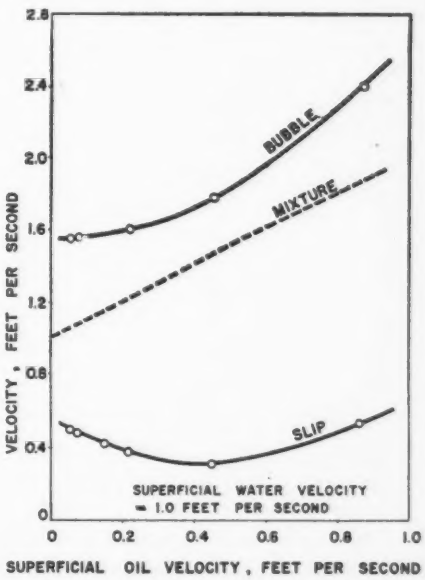

Figure 9—Effect of oil velocity on bubble velocity.

velocity of 0.39-ft./sec. to 0.53-ft./sec. at a mixture velocity of 1.87-ft./sec.

The effect of the superficial oil velocity on the bubble velocity is shown in Figure 9. In this figure also the mixture velocity has been given and, in addition, the variation of slip velocity with superficial oil velocity is indicated. In the region of bubble flow, which extends to an oil velocity of about 0.40-ft./sec., the bubble velocity is relatively insensitive to the oil rate. In the slug flow region, however, the influence of the oil rate on the bubble velocity becomes quite significant. The lower curve shown in Figure 9 indicates the variation in slip velocity with superficial oil velocity. It is interesting to note that this relationship passes through a minimum at about the bubble-slug transition.

Figure 10 shows a first estimate of bubble size distribution for a superficial oil velocity of 0.154-ft./sec. at a superficial water velocity of 1.0-ft./sec. The size distribution is shown both on the basis of the number of bubbles and on the basis of the volume of bubbles. While the size distribution (on the frequency basis) should be substantially correct for the smaller diameters, there appears to be considerable error in the estimation of diameters of large bubbles. The flow rate of oil obtained from the size distribution given is approximately 30% low. This large discrepancy is not too surprising in view of the difficulty involved in estimating from a two dimensional view the equivalent diameters of the highly distorted, large bubbles.

TABLE 4

EXPERIMENTAL RESULTS

Test No.	Bubble Velocity ft./sec.	Holdup Ratio		Average Density[b] lb./ft.³	Pressure Drop lb./ft.²/ft.	Calculated Pressure Drop[c] lb./ft.²/ft.
		Observed Directly	From Bubble Velocity[a]			
18	1.60	1.45	1.38	61.1	61.7	61.6
19	1.55	1.73	1.48	61.8	62.5	62.2
26	1.55	1.67	1.61	61.9	62.3	62.3
27	0.780	2.20	2.20	61.3	61.7	61.4
28	2.40	1.52	1.29	62.0	63.2	63.1
29	1.57	1.50	1.42	61.4	62.2	61.9
31	2.40	1.44	1.55	59.0	59.8	60.1
34	1.76	1.42	1.31	59.9	60.75	60.6
35	2.30	1.44	1.44	58.8	59.8	59.9

[a]From Equation (5)
[b]From Equation (7)
[c]From Equation (9)

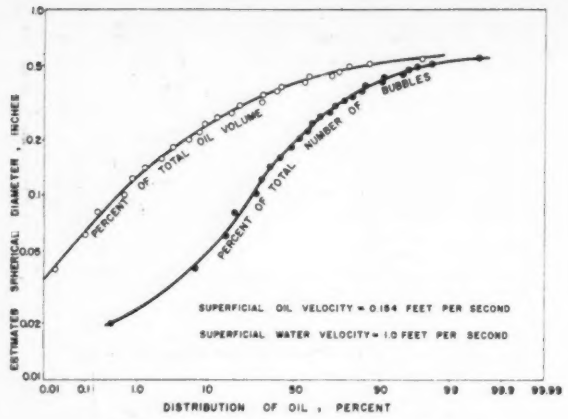

Figure 10—Size distribution of bubbles.

Discussion

High-speed motion picture photography appears to have certain advantages in the study of two-phase flows. The most prominent of these is the possibility of obtaining simultaneously the geometry and behaviour of individual flow units. The analysis of the motion pictures may be carried out quite readily if the projection equipment used has a frame counter and can operate in single frame operation. The use of a rear projection screen with a superimposed grid appears to have certain advantages for the analysis of film if sufficient accuracy can be obtained.

In earlier investigations[1] it has been assumed that the entrance section had no effect on the resulting flow which was a function only of the flow rates of the phases, the phase properties and the tube size. This assumption was based upon preliminary tests made with various entrance or mixing sections with the air-water system. It now appears possible that the entrance section may be important in some cases, particularly for immiscible liquid systems at low flow rates. It is difficult to imagine the grouping and clustering of bubbles observed at low flow rates arising if the oil were injected axially through a smaller tube. At higher flow rates, however, when the rates of shear in the mixing tee are high, the flow pattern undoubtedly is independent of the entrance section.

The good comparison of observed and calculated holdup ratios and pressure drops indicates that the assumptions made in the calculations are reasonable (and the bubble flow can, in this case, be treated as a modified slug flow). Since the frictional component is such a small fraction of the total pressure drop, the analysis of the frictional losses could be considerably in error. The theory presented should apply to any periodic flow if a characteristic velocity exists for the flow units. It is interesting to note that in all but two cases the observed holdup ratio is greater than that calculated from the bubble velocity. As the observed holdup ratio is the average for the entire vertical flow section, including the entrance section, this behavior is in agreement with the results of Moissis and Griffith[9] who predict significantly higher holdup ratios in the entrance section for slug flow. No quantitative comparison is possible, however, since their data apply to gas-liquid flow.

There are a number of possible modifications of the equipment which might make the data more valuable. For some investigations a measure of pressure or pressure gradient obtained along with the motion picture record of the flow might prove valuable. This could be obtained most easily by installing pressure transducers in the test section being photographed and connecting the output leads to an oscilloscope mounted beside the test section. There are also cameras available which will record an oscilloscope trace on the film through a separate optical system.

Another modification which is being considered at present is the installation of a mirror system to give a side view of the test section. This would be a great help in estimating bubble volumes since, as mentioned above, the bubbles are frequently not symmetrical.

As has been mentioned above, special methods of lighting may be required to outline the flow structure in some cases. This referred particularly to the use of a transverse plane of light to outline the surface of the water film on the tube wall for slug and annular flows. It may also be possible to use this technique in outlining the structure of froth flow.

Nomenclature

A_t = Cross-sectional area of tube, ft.^{2}
D = Diameter of tube, ft.
f = Friction factor, $f = \dfrac{(\Delta P/\Delta x)\, g_c D}{2\, V^2}$, dimensionless
g_c = Dimensional constant, $\dfrac{\text{ft. lb}_m.}{\text{lb}_f.\ \text{sec.}^2}$
H_R = Holdup ratio, dimensionless
L = Length along tube, ft.
$\dfrac{\Delta P}{\Delta x}$ = Pressure gradient, lb./ft.^{2}/ft.
Re = Reynolds number, dimensionless
t = Time, sec.
v = Bubble volume, cu. ft.
V = Velocity, ft./sec.
μ = Viscosity, lb$_m$./ft. sec.
ρ = Density, lb$_m$./cu. ft.

Subscripts

a = Average
b = Bubble
p, i = Bubble designation
R = Reference (water) phase
S = Second (oil) phase

Superscripts

$*$ = Time interval

References

(1) Brown, R. A. S., Sullivan, G. A., and Govier, G. W., "The Upward Vertical Flow of Air-Water Mixtures. III. Effect of Gas Phase Density on Flow Pattern, Holdup and Pressure Drop", Can. J. Chem. Eng., **38,** 62 (1960).

(2) Hughmark, G. A., "Holdup and Pressure Drop with Gas-Liquid Flow in a Vertical Pipe", Ph.D. Thesis, Louisiana State University 1959.

(3) Calvert, S., and Wililams, B., "Upward Cocurrent Annular Flow of Air and Water in Smooth Tubes", A.I.Ch.E. Journal, **1,** 78 (1955).

(4) Griffith, P., and Wallis, G. B., "Two-Phase Slug Flow", Paper presented at the A.S.M.E.-A.I.Ch.E. Heat Transfer Conference, Buffalo, N.Y., August 15-17, 1960.

(5) Laird, A. D. K., and Chisholm, D., "Pressure and Forces along Cylindrical Bubbles in a Vertical Tube", Ind. Eng. Chem., **48,** 1361 (1956).

(6) Govier, G. W., Sullivan, G. A., and Wood, R. K., "The Upward Vertical Flow of Oil-Water Mixtures", Paper presented at the A.I.Ch.E. 43rd National meeting, Tulsa, Oklahoma, September 25-28, 1960.

(7) Hyzer, W. G., "Hyzer on High Speed", Photo Methods for Industry, **3,** No. 7, 57 (1960) and **3,** No. 8, 59 (1960).

(8) Wood, R. K., "The Upward Vertical Flow of Oil-Water Mixtures", M.Sc. Thesis, University of Alberta, 1960.

(9) Moissis, R., and Griffith, P., "Entrance Effects in Developing Slug Flow", Technical Rept. No. 18 NONR-1941 (39), DSR Project No. 7-7673, June, 1960.

★ ★ ★

Determination of Ternary Liquid-Liquid Systems by Use of the Lever Rule[1]

E. L. HERIC[2] and KENNETH R. WILLIAMS[3]

A method is described for the determination of ternary liquid-liquid systems. The approach is based upon a combination of the lever rule and the measurement of a physical property which is a function of composition. The method has been tested upon the system toluene-water-acetic acid at 25 ± 0.05° and found to yield results in agreement with literature values. A possible modification of the method—which may be necessary in systems where tie-lines are essentially parallel when expressed on the usual weight per cent basis—is described.

The traditional method of study of ternary liquid-liquid systems is that of "cloud point" titration[1]. For precise results this technique is tedious, and, moreover, there are at least two inherent disadvantages to the method: (a) one cannot explicitly fix a point on the binodal curve, but only reckon that it must lie between two limits, one representing the appearance and the other the disappearance of a second phase; (b) the appearance of the second phase may be uncertain in that its form may vary even in a given system[2]. The subjectivity of this method may be avoided by use of the procedure described by Prutton et al[3], although the latter may be somewhat laborious in that it requires a relatively large number of known synthesized mixtures. An alternative to the above methods is presented here, which may have certain advantages; the number of weighing operations is not large, yet it is possible to fix with the same series of known synthesized mixtures both the binodal curve and the tie-lines. The method involves use of the lever rule[4] in combination with measurements of a suitable physical property which varies continuously over the binodal curve.

To facilitate explanation of the present method it is described in terms of the system toluene-water-acetic acid; this was studied as a means of determining the practicality of the method. No tabulation of results obtained by the present method is presented, as the agreement only confirms the previously reported values[5]. To summarize, results of both studies agree to the extent that the average departure of the binodal points obtained by the present method is ± 0.1 weight % from the smoothed curve drawn through the literature values. Present and literature tie-line data also are in quite good agreement.

[1]*Manuscript received December 22, 1960; accepted April 8, 1961.*
[2]*Associate Professor, Department of Chemistry, University of Georgia, Athens, Georgia, U.S.A.*
[3]*Graduate Student, Department of Chemistry, University of Georgia, Athens, Georgia, U.S.A.*
Based on a paper presented at the Southeastern Regional Meeting of the American Chemical Society, Birmingham, Alabama, November 5, 1960.

The Method

For best application of the method it is advisable to have an idea of the general nature of the system to be studied. This need consist only of the approximate location, perhaps to the nearest whole % by weight, of three points on the binodal curve, namely, the plait point and the mutual solubilities of the two non-consolute liquids, respectively C, D_U and D_L in Figure 1*. The cloud point method may be used to advantage for this purpose; for such approximate work it is rapid and the objections noted above are not pertinent. The plait point was located by alternately adding each of the three components to an initial known toluene-water mixture so as to maintain about equal volumes of the two phases until the system abruptly became homogeneous. The approach to the plait point is accompanied by a convergence of the densities of the two phases; this effect serves as a useful indicator of the point's proximity.

After fixing the locations of these points, an estimate of the binodal curve was made, the dashed line in Figure 1. On this basis two series of *heterogeneous* mixtures were prepared. The first series, "reference mixtures", indicated by points R_{1XY}, R_{2XY} and R_{3XY} was prepared by adding variable known amounts of the homogeneous mixture (X) of toluene and acetic acid to known amounts of heterogeneous mixtures (Y) of toluene and water. X and Y were selected so that the straight line, XY, joining these two points — the line upon which all mixtures formed from them must lie — would pass through the binodal curve near the plait point and on that side of it which contains phases richer in the same non-consolute making up the major part of Y. The purpose of this selection, as will be evident below, was to allow the determination of the system over all ranges of concentration, including that near the plait point. X and Y should also be selected so that even without using overly large amounts of the components there will be sufficient quantities of both phases of each reference mixture for the procedures to be described.

The second series of known mixtures, "scanning mixtures," indicated by points S_4, S_5 and S_6, was to lie in the region toward the portion of the binodal curve opposite the reference mixtures. Scanning mixtures need not fall on a common line, but again there should be sufficient amounts of both phases of each mixture as noted above.

After allowing the various thermostated mixtures to reach equilibrium after agitation, a sample of each phase was removed

*Throughout this work, letter subscripts refer to various specific points. In this instance, U and L refer respectively to the upper and lower phases on the base tie-line. Number subscripts refer to the tie-lines upon which points fall when such identification is necessary. Letter superscripts refer to a coordinate of a point in terms of the component indicated.

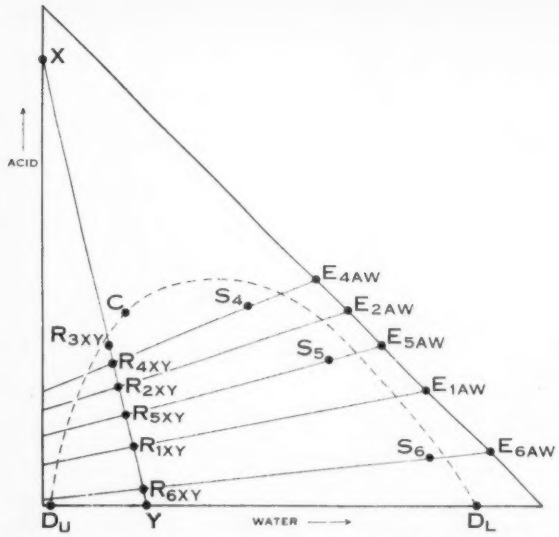

Figure 1—Reference, scanning and extrapolated mixtures.

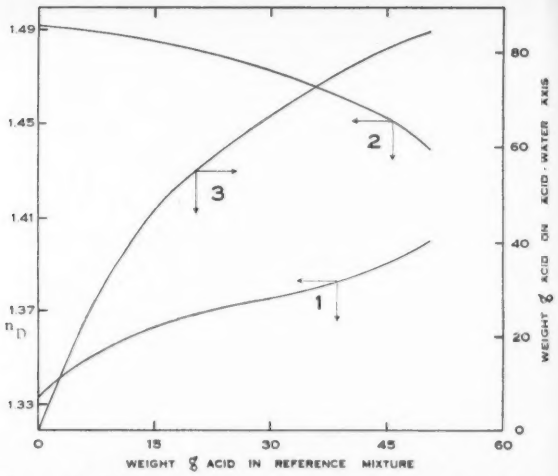

Figure 2—Working plot for the determination of tie-line slopes.

(1) n_D versus weight % acid in reference mixture, water-rich phase.

(2) n_D versus weight % acid in reference mixture, toluene-rich phase.

(3) weight % acid in reference mixture versus weight % acid on acid-water axis.

and the refractive index measured with a Bausch and Lomb precision refractometer. It was now possible to construct the first two plots shown in Figure 2. These are plots of n_D versus weight % acetic acid for reference mixtures. The curves are two branches, each corresponding to one side of the binodal curve. These plots in effect fix one point on each tie-line of the system, namely, that point upon the line XY in Figure 1. (In reality only one phase of the heterogeneous region need be considered, but a study of both phases provides a rapid means of duplicate determination and appears to be worthwhile.) The two plots were combined with the refractive indices of scanning samples in constructing the third plot in Figure 2, by means of which a second point on each tie-line may be located. This is equivalent to the establishment of the slopes of the tie-lines. The third plot has been formulated in terms of weight % acetic acid on the acid-water axis versus weight % acetic acid for the reference mixture which falls on the same tie-line. The only significance of the first of these functions is that is shows where the tie-lines would intersect the acid-water axis if they were extended beyond the binodal curve.

Establishment of points used in constructing the third plot is based upon the fact that any two points on the same tie-line yield the same pair of phases at equilibrium. Thus for mixture S_4 in Figure 1 the refractive indices of the two phases corresponded to those of a point R_{4XY} interpolated from the first two plots in Figure 2. By passing a straight line through points S_4 and R_{4XY} in Figure 1 it is possible to fix point E_{4AW} on the acid-water (AW) axis, an "extrapolated mixture". Points E_{5AW} and E_{6AW} are similarly fixed using the pairs $S_5 - R_{5XY}$ and $S_6 - R_{6XY}$. The extrapolation may be performed either graphically or algebraically[6]. In passing, it should be noted that, after the third plot of Figure 2 has been constructed, it in turn may be used to fix corresponding pairs of points such as $R_{2XY} - E_{2AW}$ and $R_{1XY} - E_{1AW}$ in Figure 1, thus defining additional tie-lines in the system.

The basis for location of the binodal curve points is the lever rule, applied in a manner similar to one previously described[7]. Assume a known heterogeneous mixture, I_1 in Figure 3. At equilibrium the mixture will exist as two phases, an upper phase I_{1U} and a lower phase I_{1L}, the location of which is the present aim. It should be noted that mixtures such as I_1 need not be in addition to those described as reference or scanning mixtures above, but may be either of the latter if sufficient amounts of them are available for the procedure to be described. This convenience is an advantage of the present method.

Determination of n_D values of the phases I_{1U} and I_{1L} is sufficient to fix the tie-line upon which these points lie. Let a working mixture of known composition, J in Figure 3, now be added to a known amount of a sample of phase I_{1U}, and the resulting mixture F_2 allowed to reach equilibrium. The choice of J is quite arbitrary except that it should cause F_2 to lie in the heterogeneous region. J may be a three- or two-component mixture, or even one of the pure components, whichever appears to be the most convenient. After F_2 has reached equilibrium, measurement of n_D of each phase, F_{2U} and F_{2L}, establishes the tie-line upon which F_2 lies.

Suppose that a weight $g_{I_{1U}}$ of phase I_{1U} has been added to a weight g_J of J. Let there be defined

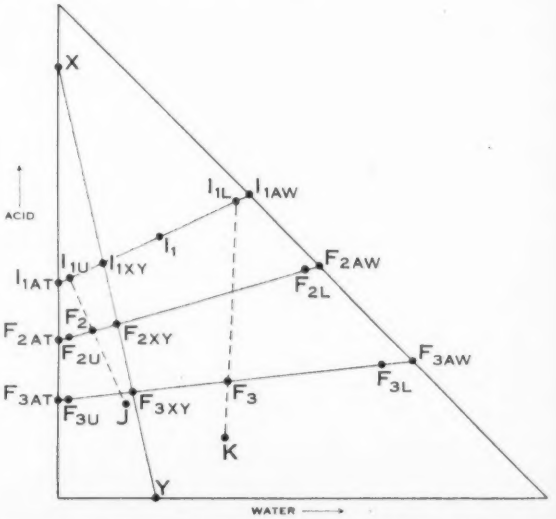

Figure 3—Illustration of the basis for determination of points on the binodal curve. All ternary points are in the heterogeneous region of the phase diagram.

$$G \equiv \frac{g_{I_{1U}} + g_J}{g_{I_{1U}}} \quad \ldots\ldots(1)$$

Now, as[7]

$$\frac{g_{I_{1U}} + g_J}{g_{I_{1U}}} = \frac{\overline{JI_{1U}}}{\overline{JF_2}} = \frac{I_{1U}{}^A - J^A}{F_2{}^A - J^A} \quad \ldots\ldots(2)$$

where the bar indicates the length of the line joining the indicated pair of points, it follows that

$$G = \frac{I_{1U}{}^A - J^A}{F_2{}^A - J^A} \quad \ldots\ldots(3)$$

Thus if straight lines are drawn from point J to intersect the tie-lines containing I_{1U} and F_2, only that single line passing through both of the latter points will yield the values of the A coordinates required by Equation (3). The desired line is established by a trial-and-error procedure.

Although the method may be applied in an essentially graphical manner, it is pertinent to express the relationships analytically, also. This provides an approach which is not subject to some of the practical limitations of graphical procedures. The tie-line upon which I_1, and thus I_{1U} and I_{1L}, lie may be defined by the linear equation

$$I_1{}^A = M_1 I_1{}^W + B_1 \quad \ldots\ldots(4)$$

where M_1 and B_1 are respectively the slope and intercept. In terms of quantities indentified in Figures 2, 3

$$M_1 = \frac{I^A{}_{1AW} - I^A{}_{1XY}}{I^W{}_{1AW} - I^W{}_{1XY}} \quad \ldots\ldots(5)$$

and

$$B_1 = I^A{}_{1AT} \quad \ldots\ldots(6)$$

In turn, for use in Equation (5) the relationships

$$I^W{}_{1AW} = 100 - I^A{}_{1AW} \quad \ldots\ldots(7)$$

and

$$I^W{}_{1XY} = (X^A - I^A{}_{1XY}) \frac{Y^W}{X^A} \quad \ldots\ldots(8)$$

are available. As Equation (8) is used repeatedly in the study of a system, it is pertinent to point out that all quantities except $I^A{}_{1XY}$ are constant once X and Y have been selected for the system. For the tie-line containing $F^A{}_2$ there are the following relationships, corresponding to Equations (4) - (8) above:

$$F^A{}_2 = M_2 F^W{}_2 + B_2 \quad \ldots\ldots(9)$$

$$M_2 = \frac{F^A{}_{2AW} - F^A{}_{2XY}}{F^W{}_{2AW} - F^W{}_{2XY}} \quad \ldots\ldots(10)$$

$$B_2 = F^A{}_{2AT} \quad \ldots\ldots(11)$$

$$F^W{}_{2AW} = 100 - F^A{}_{2AW} \quad \ldots\ldots(12)$$

$$F^W{}_{2XY} = (X^A - F^A{}_{2XY}) \frac{Y^W}{X^A} \quad \ldots\ldots(13)$$

If, now, Equation (14), comparable to Equation (3) above,

$$G = \frac{I^W{}_{1U} - J^W}{F^W{}_2 - J^W} \quad \ldots\ldots(14)$$

is combined with Equations (3), (4), and (9), there is obtained Equation (15) explicit in $I^A{}_{1U}$:

$$I^A{}_{1U} = \frac{M_1[(G-1)(J^A - M_2 J^W) - GB_2] + M_2 B_1}{M_2 - M_1} \quad \ldots\ldots(15)$$

The last equation is in terms of known parameters of the system. A second coordinate of the binodal point, $I^W{}_{1U}$, may be obtained from Equation (4).

Figure 3 also contains points associated with the location of I_{1L}, the lower phase of mixture I_1, by the addition of a working mixture K to obtain a point F_3 in a manner quite parallel to that just described for the location of I_{1U}. If, corresponding to G in Equation (1), there is now defined

$$G' \equiv \frac{g_{I_{1L}} + g_K}{g_{I_{1L}}} \quad \ldots\ldots(16)$$

where the subscripts are now pertinent to the points I_{1L}, F_3 and K, it can be shown that, corresponding to Equations (3) and (15),

$$G' = \frac{I^A{}_{1L} - K^A}{F^A{}_3 - K^A} \quad \ldots\ldots(17)$$

and

$$I^A{}_{1L} = \frac{M_1[(G'-1)(K^A - M_3 K^W) - G'B_3] + M_3 B_1}{M_3 - M_1} \quad \ldots\ldots(18)$$

Point I_{1L} may thus be located graphically by trial-and-error methods with Equation (17), or analytically with Equation (18). It should be noted that there is no fixed relationship between the tie-lines containing respectively points F_2 and F_3, as each is dependent only upon the relative amounts of I_{1U}, I_{1L}, J or K used.

Aside from difficulties inherent in the use of graphical procedures for precise results, the limiting aspect of the present method is implicit in the denominators of the functions in Equations (15) and (18). As M_2 or M_3 approaches M_1, that is, as the tie-lines approach parallelism, the uncertainty in the A coordinate of a binodal curve point approaches infinity. This may be predicted, of course, purely from the geometry of parallel lines. It can be shown, however, from the relation between an angle and its tangent, that a difference in slope of only six degrees between the two tie-lines used in establishing a binodal point is sufficient to reduce the uncertainty in the latter to about $\pm$ 0.03 weight %. The uncertainty decreases as the slopes become more unlike, becoming, for example, about $\pm$ 0.01 weight % when the difference is 17 degrees. In stating these uncertainties some assumptions have been made concerning the precision of measurements. First, the compositions of synthesized mixtures should be known to the nearest 0.01 weight %. This requirement is quite readily satisfied even in the preparation of mixtures of pre-selected composition, Y in Figure 2, by the use of microliter pipets for final adjustments. Second, weights of I_{1U}, I_{1L}, J or K in Figure 3 should be determined to 1 part in 20,000. These requirements concerning weights and compositions mean that the volume of the vapor phase must be kept small, or that it must be possible to correct for the weights of the components in the vapor phase. Finally a G value of no more than about 1.5 should be used if extrapolation errors inherent to such a method are not to become overly large.

It is evident that, even though the method as described would be applicable to many systems, its usefulness would be increased if it could be applied to systems where tie-lines show only a small departure from parallelism on the usual weight % plot. While this complication was not a factor in the system described here, the consequences have been considered in anticipation of such a problem. A possible solution to this problem lies in a transformation of concentration variables from weight % to mole % at a certain stage in the procedure. Such a transformation will produce a spectrum of tie-line slopes in these systems when there is a significant difference between the molecular weights of the non-consolute components.

In modifying the method as previously described on the basis of weight %, no change need be made until the aspects of Figure 3 are considered. Up to that point use of weight % is quite acceptable, and undoubtedly more convenient. Consider Figure 3 again, but now visualize that each designation refers to mole %. To distinguish between the previous interpretation of Figure 3 and that now to be assumed, suppose that all of the labelled points are altered from upper to lower case letters —

the latter to indicate the same quantities as before but now in terms of mole rather than weight %. Thus, for example, the equation of the tie-line containing i_1 may be written as

$$i^A{}_1 = m_1 i^W{}_1 + b_1 \quad \ldots\ldots(19)$$

where m_1 and b_1 are respectively the slope and intercept. Other equations similar to those stated in terms of weight % may be listed, and the present modification of binodal point determination carried out in a manner which is essentially analytical as described above. This will not be done, however, because the modification is such that the resulting equations whose purpose is that of Equations (15) and (18) are too cumbersome to be of practical value. Thus the present discussion will be confined to a graphical solution of the problem.

To evaluate b_1, one notes that

$$b_1 = i^A{}_{1AT} = \frac{100\,\dfrac{I^A{}_{1AT}}{\underline{M}_A}}{\dfrac{I^A{}_{1AT}}{\underline{M}_A} + \dfrac{I^T{}_{1AT}}{\underline{M}_T}} = \frac{\underline{M}_T}{\dfrac{\underline{M}_T - \underline{M}_A}{100} + \dfrac{\underline{M}_A}{B_1}} \quad \ldots\ldots(20)$$

where $\underline{M}$ is the molecular weight of the indicated component. m_1 may then be evaluated in terms of b_1 and $i^A{}_{AW}$, as

$$m_1 = \frac{i^A{}_{1AW} - b_1}{100 - i^A{}_{1AW}} \quad \ldots\ldots(21)$$

A useful substitution for $i^A{}_{1AW}$ in Equation (21) is

$$i^A{}_{1AW} = \frac{100\,\dfrac{I^A{}_{1AW}}{\underline{M}_A}}{\dfrac{I^A{}_{1AW}}{\underline{M}_A} + \dfrac{I^W{}_{1AW}}{\underline{M}_W}} = \frac{\underline{M}_W}{\dfrac{\underline{M}_W - \underline{M}_A}{100} + \dfrac{\underline{M}_A}{I^A{}_{1AW}}} \quad \ldots\ldots(22)$$

Equations (20) and (21) thus provide the means whereby the convenience of working on a weight % basis may be preserved until Equation (19) is required.

It will be apparent that equations in terms of point f_2 similar to those above for point i_1 may be stated. Thus

$$f^A{}_2 = m_2 f^W{}_2 + b_2 \quad \ldots\ldots(23)$$

$$m_2 = \frac{f^A{}_{2AW} - b_2}{100 - f^A{}_{2AW}} \quad \ldots\ldots(24)$$

and

$$b_2 = \frac{\underline{M}_T}{\dfrac{\underline{M}_T - \underline{M}_A}{100} + \dfrac{\underline{M}_A}{B_2}} \quad \ldots\ldots(25)$$

As a transformation to mole % has occurred, it is appropriate to modify the approach of Equations (1) - (3) to

$$N \equiv \frac{n_{i_{1U}} + n_j}{n_{i_{1U}}} = \frac{i^A{}_{1U} - j^A}{f^A{}_2 - j^A} \quad \ldots\ldots(26)$$

where n_j and $n_{i_{1U}}$ refer respectively to the number of moles of j added to i_{1U}. Unlike Equation (3), however, Equation (26) by itself is insufficient to locate i_{1U} because $n_{i_{1U}}$ is an unknown quantity. The solution to this difficulty may be found in the addition of another step to the procedure beyond that required for the use of Equation (3). This consists of the addition of a second working mixture of a known composition, such as h, to another sample of i_{1U} to achieve another point f_4. Points f_2 and f_4 will not ordinarily lie on the same tie-line, except by coincidence. It will be apparent that equations in terms of f_4 similar to (23-25) above may be written.

In the following, the restriction will be placed that neither j nor h is to contain any of that component whose concentration is used as the means of fixing the binodal points, i.e., in the present system, acetic acid. This restriction is necessary to obtain the resulting relationships in a usable form, as will be seen below. Comparable to Equation (26),

$$N'' \equiv \frac{vn_{i_{1U}} + n_h}{vn_{i_{1U}}} = \frac{i^A{}_{1U} - h^A}{f^A{}_4 - h^A} \quad \ldots\ldots(27)$$

where it is assumed that the sample of i_{1U} to which h is added is v times as heavy as the one to which j was added.

If to n_A moles of acid which are present in the mixture totalling $n_{i_{1U}}$ moles there is added j containing n_T moles of toluene and n_W moles of water, then

$$f^A{}_2 = 100\,\frac{n_A}{n_{i_{1U}} + n_T + n_W} \quad \ldots\ldots(28)$$

and

$$N = \frac{n_{i_{1U}} + n_T + n_W}{n_{i_{1U}}} \quad \ldots\ldots(29)$$

Let the amount of h added contain pn_T moles of toluene and qn_W moles of water. Then

$$f^A{}_4 = \frac{100\,vn_A}{vn_{i_{1U}} + pn_T + qn_W} \quad \ldots\ldots(30)$$

and

$$N'' = \frac{vn_{i_{1U}} + pn_T + qn_W}{vn_{i_{1U}}} \quad \ldots\ldots(31)$$

Finally from Equations (34) and (37)

$$\frac{N'' - 1}{N - 1} = z \quad \ldots\ldots(32)$$

where

$$z = \frac{pn_T + qn_W}{v(n_T + n_W)} \quad \ldots\ldots(33)$$

Point i_{1U} may thus be located by striking straight lines from points j and h, which lines are to pass respectively through f_2 and f_4 and intersect at a point on the tie-line containing i. The procedure has an obvious resemblance to that described for the weight % basis, except that Equation (32) must also be satisfied.

It appears that, due to the larger number of steps involved, the mole % method is not capable of the best results obtainable on the weight % basis. The former would be preferable to the latter, however, when the complication of parallel tie-lines arises on the weight % basis.

Acknowledgement

Acknowledgement is made to the donors of the Petroleum Research Fund, administered by the American Chemical Society, for support of this research.

Nomenclature

A	=	acetic acid
B	=	tie line intercept, wieght % basis
b	=	intercept of tie-line, mole % basis
C	=	plait point
D	=	mutual solubility of water and toluene
E	=	extrapolated mixture, hypothetical
F	=	mixture formed by addition of $J(K)$ to upper (lower) phase of I, weight % basis
f	=	mixtures formed by addition of either j or h to upper phase of i, mole % basis
G	=	function (Equation (1)) of weights of J and upper phase of I
G'	=	function (Equation (16)) of weights of K and lower phase of I
g	=	weight of a quantity of a component or mixture
h	=	working mixture (contains no acid) used in establishing composition of upper phase of i, mole % basis
I	=	mixture lying on tie-line containing binodal points which are to be established experimentally, weight % basis
i	=	mixture lying on tie-line containing binodal points which are to be established experimentally, mole % basis
J,K	=	working mixtures used in establishing composition of upper and lower phases of I, weight % basis
j	=	working mixture (contains no acid) used in establishing composition of upper phase of i, mole % basis
L	=	lower phase of heterogeneous mixture
M	=	slope of tie-line, weight % basis

$\underline{M}$ = molecular weight
m = slope of tie-line, mole % basis
N = function (Equation (26)) of moles of j and upper phase of i
N'' = function (Equation (27)) of moles of h and upper phase of i
n = moles of a quantity of a component or mixture
p,q = weight of toluene (water) in quantity of h added to fraction of upper phase of i/weight of toluene (water) in quantity of j added to fraction of upper phase of i
R = reference mixture, prepared synthetically
S = scanning mixture, prepared synthetically
T = toluene
U = upper phase of heterogeneous mixture
v = weight of fraction of upper phase of i added to h/weight of fraction of upper phase of i added to j
W = water
X,Y = working mixtures used in preparing R
z = function (Equation (33)) of p, q, v and the moles of toluene and water in the quantity of j added to the upper phase of i

References

(1) Bowden, S. T., "The Phase Rule and Phase Reactions", Macmillan and Co., Ltd., London, 1954, pp. 253-4.
(2) Denzler, C. G., J. Phys. Chem., **49,** 363 (1945).
(3) Prutton, C. F., Walsh, T. J., and Desai, A. M., Ind. Eng. Chem., **42,** 1212 (1950).
(4) Miller, W. L., and McPherson, R. H., J. Phys. Chem., **12,** 710 (1908).
(5) Woodman, R. M., J. Phys. Chem., **30,** 1283 (1926).
(6) Hill, A. E., and Ricci, J. E., J. Am. Chem. Soc., **53,** 4305 (1931).
(7) Heric, E. L., and Rutledge, R. M., Can. J. Chem. Eng., **38,** 46 (1960).

★ ★ ★

NOTE TO THE EDITOR

A Generalized Method for the Estimation of Heat of Vaporization

CARL ST. PIERRE and CHI TIEN
Department of Chemical Engineering,
Essex College,
Assumption University of Windsor, Windsor, Ont.

A number of methods have been proposed for the prediction of heat of vaporization. However, most of these suggestions deal with a rather limited class of substances and in some cases it requires at least one value of the heat of vaporization at a given temperature and therefore is not generalized in the true sense. A recent paper by Kunte and Doraiswamy[1] gave a correlation and claimed excellent accuracy. Unfortunately there seems to have been some doubt about the validity of its mathematical derivation and furthermore the computed value of λ_c is found to be increasing with the increase of temperature (contrary to Trouton's rule).

The present communication aims at presenting a generalized method for estimating the heat of vaporization. As a starting point, the Clausius-Clapeyron equation as written in terms of compressibility factor is used. This is given as:

$$\frac{\lambda_s}{T_c} = \frac{R T_{r_s}^2 (Z_{s_G} - Z_{s_L})}{P_{r_s}} \left(\frac{\partial P_r}{\partial T_r}\right)_s \quad \ldots\ldots\ldots\ldots (1)$$

The heat of vaporization, λ, refers to that at the saturation condition. Riedel's expression for vapor pressure is used for the evaluation of $\left(\frac{\partial P_r}{\partial T_r}\right)$. This is found to be:

$$ln\ P_r - \alpha\ ln\ T_r - 0.0838\ (\alpha - 3.75)\ (36/T_r - 35 - T_r^6 + 42\ ln\ T_r) \quad \ldots\ldots (2)$$

and

$$\frac{\partial P_r}{\partial T_r} = P_r[\alpha/T_r + 0.0838\ (\alpha - 3.75)\ (36/T_r^2 + 6T_r^5 - 42/T_r)] \quad \ldots\ldots\ldots (3)$$

where α is the slope of the vapor pressure curve at the critical point.

Substituting (3) into (1), we obtain the expression for α at the saturation condition:

$$(\lambda/T_c)_s = R(Z_{s_G} - Z_{s_L})\ [\alpha T_{r_s} + 0.0838\ (\alpha - 3.75)\ (36 + 6T_{r_s}^7 - 42T_{r_s})]$$

Numerical values of Z_{s_G} and Z_{s_L} for specified values of T_{r_s} and P_{r_s} are given by Lyderson et al[2] for values of $Z_c = 0.23$, 0.25, 0.27 and 0.29. Values of α for different Z_c can be found from Reference (3). With this information, values of $(\lambda/Tc)_s$ for a given Z_c can be computed at various saturation conditions.

For the values of (λ/T_c) at temperatures other than the saturation conditions, the Trouton's rule is used to account for the temperature effect, namely:

$$\frac{\lambda}{\lambda_s} = \left[\frac{1 - T_r}{1 - T_{r_s}}\right]^{0.38}$$

From Equations (4) and (5), it can be seen that the numerical values of λ/T_c is a function of three parameters, T_r, P_r and Z_c. For any given value of Z_c, values of λ/T_c are plotted against T_r using P_r as parameter. Figure 1 gives the result of calculation. As an indication of the reliability of this method, experimental values of λ/T_c for a number of compounds are compared with the values obtained from the graph. The accuracy is not as good as hoped. However, with the exception of chlorine,

TABLE 1

COMPARISON BETWEEN EXPERIMENTAL AND PREDICTED VALUES OF λ (λ) at boiling point (cal./ml.)

Compound	Z_c	Boiling Point °K.	Experimental	Predicted	% Diff.
Argon[2]	0.29	87.2	1,596	1,615	+1.6
Chlorine[2]	0.276	238.9	4,878	5,660	+14
Carbon Dioxide[2]	0.28	194.6	6,030	4,020	−33
Hydrogen Chloride[2]	0.27	188	3,860	4,530	+17.3
Hydrogen Sulfide[2]	0.28	212.7	4,463	4,410	−1.2
Carbon Tetrachloride[1]	0.27	349.7	7,170	7,400	+3.2
Sulfur Trioxide[1]	0.26	316.3	9,990	7,300	−27
Sulfur Dioxide[1]	0.27	263	5,950	5,880	−1.2
Oxygen[2]	0.29	90	1,629	1,640	+0.7
Carbon Monoxide[2]	0.29	81.5	1,444	1,385	−4.1
Nitrogen[2]	0.29	77.2	1,336	1,310	−2.0
Freon[1]	0.27	242.5	4,850	5,100	+5.2
Carbon Disulfide[1]	0.29	319.2	6,400	5,970	−6.7
Hydrogen Cyanide[2]	0.29	298.7	6,027	7,350	+21

Source of information:
[1]Selected Values of Chemical Thermodynamic Properties, July 1953
[2]Chemical Engineers Handbook, 3 ed. McGraw-Hill Book Co. 1950

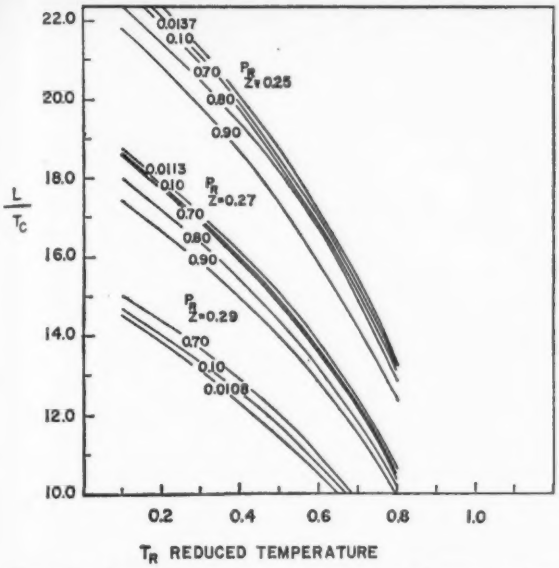

Figure 1—Generalized chart for latent heat of vaporization.

carbon dioxide, sulfur trioxide and hydrogen cyanide, it does give a fairly reasonable estimate. Table 1 summarized the results of comparison.

Nomenclature

P_r = reduced pressure
R = gas law constant
T_c = critical temperature
T_r = reduced temperature
Z = compressibility factor
a = slope of the vapor pressure curve at critical point
λ = heat of vaporization

Subscripts:

s = saturation state
g = vapor state
l = liquid state

References

(1) Kunte, M. V., and Doraiswamy, L. K., Chem. Eng. Sci. **12,** 1 (1960).

(2) Lyderson, A. L., Greenkorn, R. A. and Horgen, O. A., "Generalized Thermodynamic Properties of Pure Fluids", Engineering Experimental Station Report No. 4, University of Wisconsin, 1955.

(3) Hougen, O. A., Watson, K. M., and Rogatz, R. A., Chemical Process Principles, Vol. II, J. Wiley (1959).

★ ★ ★

Pilot Plant Unit for the Continuous Methanolysis of Glyceride Oils[1]

P. M. JANGAARD[2] and F. A. VANDENHEUVEL[3]

Efficient continuous methanolysis using an alkaline catalyst is achieved in the simple system described.

At 100°C., in one hour, a volume of oil equal to six times the free volume of the reactor is converted to methyl esters.

Un reacteur simple à haut rendement horaire pour la méthanolyse continue en milieu alcalin est décrit.

A 100°C. le volume d'huile convertie par heure égale 6 fois le volume libre du réacteur.

A three-step process for the production from herring oil of methyl ester fractions having specific properties was described by the authors in 1957[1]. The process comprised: first, the production of mixed methyl esters by methanolysis of the oil; second, their fractionation by solvent segregation; and third, the fractional distillation of the segregated ester fractions. Since steps 2 and 3 lend themselves to continuous operation, it seemed desirable, both from the point of view of economy and of simplicity, to integrate the three steps in one continuous process. Continuous methanolysis was therefore investigated.

The reaction expressed by the following equation

$$\text{Triglyceride} + \text{methyl alcohol} \overset{OH^-}{\rightleftharpoons} \text{glycerol} + \text{methyl esters}$$

had been known for many years as a typical example of alcoholysis. As such it had been described and discussed in several articles which have been reviewed recently by Kaufmann *et al*[2], and by Poré[3].

In many laboratories, the reaction was applied to batch type operations only. The authors themselves had used extensively the conditions described by Bradshaw and Meuly[4] whereby over 95% of a glyceride oil can be converted to methyl esters in about one hour. The reaction was carried out at 60°C. using 75% excess methanol and 0.5% NaOH as the catalyst.

The above conditions had been found very satisfactory in promoting the separation from the final reaction mixture of two immiscible phases, the methyl ester layer and the glycerol layer, thereby simplifying the recovery of the products. Increasing the excess methanol beyond 100% was observed to interfere with this separation, and likewise, concentrations of the catalyst above 1% were found to complicate subsequent operations.

It was thought that a simple solution to the problem of continuous methanolysis might consist of pumping metered amounts of the reagents through a heated channel allowing sufficient time of contact for a satisfactory degree of methanolysis to develop in the mixture.

Evidently, the efficiency of such a system would be increased by an increase of the reaction rate. For the reasons given above, means of attaining this result were restricted insofar as excess methanol and amount of catalyst were concerned. The effects of an elevation of the temperature, on the other hand, were unknown.

The results of kinetic study of the reaction, which will be presented in detail elsewhere, indicate the following useful facts.

An appreciable increase in reaction rate can be achieved by operating at higher temperature. In Figure 1 is shown a curve expressing the relationship between the temperature and the time required to promote 90% release of the glycerol from herring oil using 0.5% NaOH and 70% excess methanol. It was found that the final equilibrium composition did not change within the range of temperature explored. Under the conditions just described, a maximum release of the glycerol corresponding to 95% was obtained in less than 7 minutes at 120°C.

The reaction was also found to involve the consecutive equilibria described by the following equations.

$$\text{Triglyceride} + \text{MeOH} \overset{OH^-}{\rightleftharpoons} \text{diglyceride} + \text{methyl ester}$$

$$\text{Diglyceride} + \text{MeOH} \overset{OH^-}{\rightleftharpoons} \text{monoglyceride} + \text{methyl ester}$$

$$\text{Monoglyceride} + \text{MeOH} \overset{OH^-}{\rightleftharpoons} \text{glycerol} + \text{methyl ester}$$

As these equations indicate, percentage conversion to methyl ester will be higher than percentage glycerol release.

It was also found that continuous agitation of the reaction mixture did not decrease the time required to reach final equilibrium. Indeed, no agitation is necessary after an initial thorough mixing of the reagents.

In designing the simple unit described below, we gave the reactor dimensions estimated to correspond to an output of 225 g. methyl esters per minute at 110°C., in order to match the capacity of the solvent segregation unit used in the following step of our process[1].

[1]*Manuscript received November 4, 1960; accepted March 20, 1961.*
[2]*Fisheries Research Board of Canada, Technological Station, Halifax, N.S.*
[3]*Department of Agriculture, Animal Research Institute, Ottawa, Ont.*
Contribution from the Fisheries Research Board, Technological Station, Halifax, N.S.

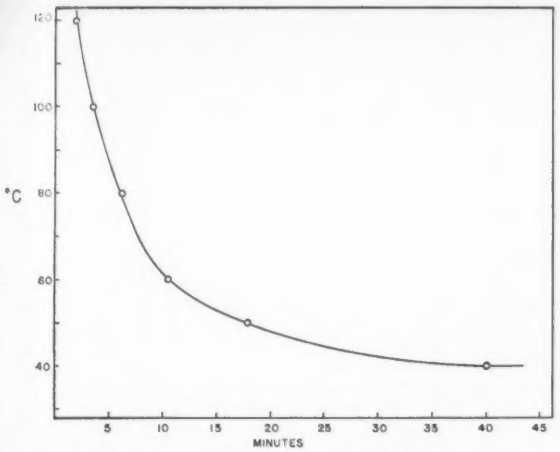

Figure 1—Curve expressing the relationship between the temperature and the time required to promote 90% release of the glycerol from herring oil using 0.5% NaOH and 70% excess methanol.

Allen and Kline have patented a procedure for the continuous methanolysis of glyceride oils[5], a general purpose continuous reactor has been patented[6], and a continuous laboratory unit for the conversion of acidulated soapstock using acid catalyst was described by Eaves *et al.*[7].

Description of the Unit

As shown in Figure 2, a solution of the catalyst in absolute methyl alcohol is contained in tank A. This solution, and the oil stored in tank B are pumped simultaneously through the system, respectively by pumps C and D. The latter are actuated by a common adjustable speed motor drive E. The liquids are mixed in F where they form an emulsion. F is a shallow circular box containing a magnetic stirrer actuated by a motor-driven external magnet. The bolted lid of this box is fitted with a thick glass window allowing visual inspection for proper adjustment of the stirring speed. The latter should be sufficient to emulsify the mixture and maintain the box full of emulsion. The reaction mixture reaches preheating coil G, a 50-ft. length of coiled ¼-in. internal diameter stainless steel tubing. This is followed by H, the reactor proper, a 50-ft. length of coiled ¾-in. internal diameter stainless steel tubing filled with small glass Raschig rings, the function of which is to promote efficient heat exchange through agitation. Both coils are immersed in oil bath I, which is equipped with electric immersion heaters, stirrer, temperature indicator and bimetallic thermoregulator. The latter, connected to a relay and switch combination, allows ±0.5°C. adjustment of the bath temperature. The temperature of the reaction mixture on entering the reactor is read on the recorder connected to thermocouple R. This temperature is about 3°C. below the bath temperature.

The reaction mixture then passes through cooling coil K, 50 ft. of ¼-in. internal diameter stainless steel tubing fitted in water jacket L, the flow being adjusted to bring the product to about 25°C. Spring valve M is adjusted to a pressure appreciably above the boiling point of the reaction mixture, i.e., 20 lb. above the vapor pressure of pure methanol at the temperature of the experiment. Through valve N, the reaction mixture reaches centrifuge O (Sharples motor-driven super centrifuge) where the methyl ester phase (outlet P) and the glycerol phase (outlet Q) are separated.

Operational Data

After adjusting the bath temperature and the operating pressure (valve M), three-stage metering pumps C and D are adjusted separately (stroke length) to deliver the required amounts of oil and catalyst solution at the selected motor speed.

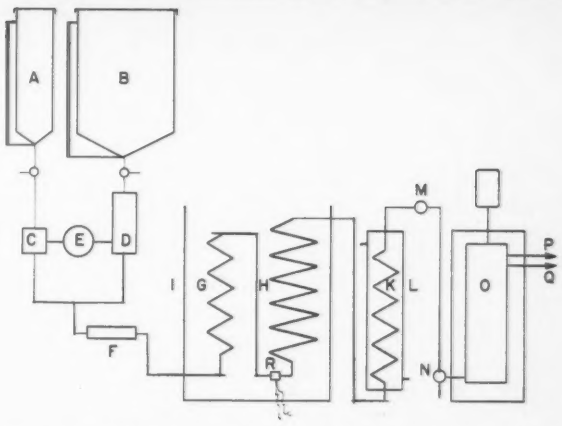

Figure 2—Pilot plant unit for the continuous methanolysis of glyceride oils.

The liquids can then be pumped in simultaneously.

A 100-ml. sample of product is collected at intervals from 3-way valve N in a container containing enough mineral acid to neutralize the catalyst. Free glycerol is then determined by a standard method on the chloroform extracted mixture[8]. Constancy of the glycerol value is observed after 30 min. Valve N can then be connected to O, and the glycerol and methyl ester phases collected separately.

Further processing of the methyl ester phase consists of vacuum stripping of the methanol it contains, and separating the small amount of soap which then precipitates. The glycerol phase is processed for the production of pure anhydrous glycerol according to a procedure which will be described in a separate article.

Our work with this unit has consisted so far in establishing its efficiency under conditions of normal production. The data thus far collected therefore do not involve a wide range of conditions.

Dried oils were used throughout these experiments since it was established that moisture will interfere very markedly with the reaction at elevated temperatures.

Some typical results shown in Table 1 have been obtained with seal oil having the following characteristics: F.F.A., 1.5%; I.V., 146; total glycerol, 10.02%. With this oil, the maximum value observed for glycerol release was 93% in a batch operation after 24 hr. at 60°C. (100% excess methanol, 0.5% NaOH).

A comparison of this result with those listed in Table 1 is legitimated by the simple rules governing equilibrium reactions. It is well known that the final equilibrium composition is unaffected by catalyst concentration. Further, the equilibrium will be displaced by a larger excess of methanol towards higher levels of conversion. Finally, it has been established, as stated

TABLE 1

GLYCEROL RELEASED FROM SEAL OIL IN RELATION TO TEMPERATURE, TIME OF CONTACT, EXCESS METHANOL, AND CATALYST CONCENTRATION

t °C.	Total flow ml./min.	Time of contact min.	Excess MeOH %	NaOH %	Free glycerol %
90	356	8.4	78	0.64	91.3
90	440	6.8	75	0.64	91.2
100	369	8.1	85	0.67	92.4
110	363	8.25	94	0.70	91.3
120	369	8.1	95	0.70	90.5

above, that the degree of conversion was unaffected by the temperature used within the range of temperature explored. For these reasons, the 93% conversion obtained after 24 hours at 60°C., undoubtedly an equilibrium value, and obtained with the largest excess methanol applied in this study, must correspond to the maximum degree of conversion attainable with this oil within the range of conditions used.

In Table 1, excess methanol is calculated as percentage over theoretical amount estimated from total bound glycerol. The catalyst used is expressed as percentage of oil weight. The time of contact is determined by dividing the free volume of the reactor (3000 ml.) by the total volume of reaction mixture flowing per minute.

It appears that a degree of conversion approaching the maximum attainable is achieved within a time of contact predictable from the kinetic data. The efficiency appears to fall to some extent when the temperature rises above 100°C. At this temperature the yield in methyl esters is about 260 gm./min. or somewhat in excess of the expected output. The volume of oil which can be treated in 24 hr. is 144 times the free volume of the reactor, an indication of the remarkable efficiency of this simple system.

References

(1) Vandenheuvel, F. A., and Jangaard, P. M., Can. Chem. Processing, **41**: 40-46 (1957).

(2) Kaufmann, R. J., Grandel, F., and Grotheus, B., Fette, Seifen, Anstrichmittel, **60**: 919-930 (1958).

(3) Poré, J., Oléagineux, **15**: 13-19, 165-172 (1960).

(4) Bradshaw, G. B., and Meuly, W. G., U.S. Patent 2,271,619 (1942).

(5) Allen, H. D., and Kline, W. A., U.S. Patent 2,383,579 (1945).

(6) Ranzenberger, W., U.S. Patent 2,832,674 (1958).

(7) Eaves, P. H., Spadaro, J. J., and Gastrock, E. A., J. Am. Oil Chemists' Soc., **36**: 230-234 (1959).

(8) Pohle, W. D., and Mehlenbacher, V. C., J. Am. Oil Chemists' Soc., **27**: 54-56 (1950).

★ ★ ★

Safety of Materials of Construction Used in Explosives Manufacture[1]

F. VAN ZEGGEREN[2]

Hazards of materials of construction in machinery used for manufacture of explosives depend on the explosive which is being handled by the machinery. Thus one has to consider the combination material/explosive as well as material and explosive themselves, in assessing hazards. Several types of hazard can occur viz., due to sparks, friction, impact or heat. For a given material the most likely factors that will influence its hazard depend on the type of hazard, e.g. for spark hazards important factors are: static pick-up of material and explosive, conductive properties and spark confinements; for impact hazards: hardness, surface roughness, elasticity, presence of cavities, confinement offered and area of contact; for frictional hazards: hardness, friction coefficient and thermal conductivity. For purely thermal hazards, only flammability need be considered.

In impact and friction the chemical action between material and explosive may play an important role. In all cases the sensitivity of the explosives themselves to the particular type of action, has to be taken into consideration. In accidental mishaps the type of hazard is often a combination of impact and friction, and requires a special test method.

In this paper the literature on some aspects of all of the above hazards is reviewed. Experimental results of frictional and frictional impact tests are discussed from a theoretical point of view. A number of results of particular interest, e.g. for aluminum alloys, coated steel and non-metallic materials are presented.

In factories where explosive materials are being handled with machinery, the hazard associated with the contacting of explosive with the various parts of the equipment, will have to be extremely slight. Such hazards will depend on a variety of factors, viz., on the type of material in contact with the explosive, on the explosive, and on a number of other conditions imposed upon the system by the type of hazard. Thus, unsafe situations can occur for different types of hazard, viz., due to sparks, friction, impact or heat. The specific safety requirements for the material to be used will, therefore, also vary.

The mechanism operative in the initiation of an explosive is not yet fully understood and many conflicting data have been reported in the literature. Although in the last decade theoretical progress has been made, the choice of materials for machinery has still been largely empirical.

A large number of test methods for materials have been devised, whose results have been interpreted as figures indicating degrees of hazard for those materials when used in a plant, but safety predictions are still rather uncertain, and progress along these lines would be welcomed.

In this paper a survey will be given of the available literature on hazards of materials in contact with explosives and several test methods and apparatus will be discussed. A number of interesting data obtained for frictional and frictional impact hazards will be viewed in the light of recent theoretical advances in the field of friction safety predictions.

Spark Hazards

If an electrically conductive body is insulated from ground, it can act as a condenser or reservoir for the accumulation of electric charge. The close approach of another conductor may bring about discharge in the form of a spark. An explosive material in the path of the spark may be ignited if it is sensitive enough and if the spark energy is high enough. Although this hazard cannot be completely excluded in explosive manufacturing machinery, the danger can be decreased considerably by adequate grounding of the conductive materials. For non-conductive materials the problem is magnified many times, since grounding is not a sufficient cure.

Also serious is the generation of static on the explosive itself. Continued rubbing leads to formation of a double layer by electron flow from the surface levels of one substance in contact with another. Rubbing of particles against the container wall, particularly if this wall is smooth, leads to very appreciable static on the particle surface[1]. The trouble can be overcome by roughening the vessel wall or by coating it with particles of the explosive material to be handled.

In all cases the sensitivity of the explosive itself to sparks is of paramount importance. Minimum spark energies have been determined for a large number of explosives[2,3]. It was found that the sensitivity increases with confinement of the explosive. For instance, unconfined nitroglycerine could not be ignited with a 12.5 Joule energy spark but when heavily confined, a 7000 ergs spark could ignite the explosive[6]. Thus confinement of spark and/or explosive should be avoided.

Prevention of static accumulation is the best safety precaution[7]. This can be effected by introducing radioactive elements[5], by roughening contact surfaces[1], or by coating the explosive particles with antistatic agents[4]. The latter method is by far preferred if the coatings do not change the required properties of the explosive.

[1]*Manuscript received January 21; accepted May 30, 1961.*
[2]*Central Research Laboratory, Canadian Industries Limited, McMasterville, Que.*
Based on a paper presented at the C.I.C. Chemical Engineering Conference, Quebec City, Nov. 7-9, 1960.

Impact Hazards

When a weight is falling down on an explosive compound, supported by a block, called an anvil, there is a chance that explosion occurs. The sensitivity of an explosive to impact is measured by this chance, usually with a so-called drop test apparatus, and is expressed in energy required to give a certain percentage of explosions (e.g., 0, 50 or 100%). Taylor and Weale[8,9] found that the hardness of the anvil was of great importance, and that a softer material required a larger fall energy, and hence is safer to use. Lack of rigidity of the anvil causes the required energy to be high, e.g. when the anvil is supported on a rubber pedestal. Thus it is preferred to keep the different machine parts as flexible as possible.

The composition of the alloy of which the falling weight consists, affects the hazard. Wöhler and Wenzelberg[10] found that when they used aluminum foil to cover up their drop testing samples, the impact hazard was increased, due to reactivity of the aluminum and the large heat of its reaction with explosive oxygen.

If the explosive, when subjected to impact, is not confined, the free falling weight will cause viscous flow in a horizontal direction. Then friction between weight and explosive takes place and surface roughness of the weight will become of importance, a rougher surface giving the more hazardous condition (see Friction Hazards).

For the same energy, a larger area of contact between falling weight and explosive reduces the probability for ignition[8]. Thus, in machinery where impacting occurs, the total energy should be distributed over as large an area as possible.

Bowden and co-workers[11] found that the presence of bubbles in explosives greatly increases their ignition probability. This was explained by a mechanism involving adiabatic compression of the bubble, and subsequent heating of the bubble and of the surrounding explosive to a temperature well above the ignition point. This mechanism also explains the behavior of a cavity in the striker, which causes the required energy to be much smaller than for a flat-ended weight. Thus cavities, and in general roughness, of materials of construction should be avoided.

Relative sensitivity measurements have been made for a large number of explosives in contact with several materials, and for a large number of materials in contact with several explosives[12]. Quantitative interpretations of these results are still completely lacking.

Friction Hazards

When two solids are rubbed together, the frictional energy is dissipated mainly in the form of heat and is concentrated in the regions of contact, which are the summits of the highest irregularities of the respective surfaces[13]. Thus hot spots of the order of 1000°C. can be formed. These high temperature flashes last for times of the order of a millisecond. When temperature and duration are high and long enough these hot spots can cause explosion in a layer of explosive between the two rubbing surfaces. Experiments on this aspect have been carried out by Bowden, Stone and Tudor[14] with nitroglycerine. The temperature rise in rubbing is given by:

$$\Delta T = \frac{\mu W v}{4a\, J\, (k_1 + k_2)}$$

where μ is the coefficient of friction, W the load between the surfaces, v the velocity of sliding, a the radius of the circular region of contact, J the mechanical heat equivalent and k_1 and k_2 the thermal conductivities of the rubbing solids. The area of contact is determined by the yield pressure (p_m) of the softer of the two materials, and since the value of the hardness (H) is usually a few percent less than the corresponding value of p_m, the above expression becomes:

$$\Delta T \sim \frac{\mu \sqrt{H}}{k_1 + k_2}$$

If one of the two materials has a much larger thermal conductivity than the other one, we get

$$\Delta T \sim \frac{\mu \sqrt{H}}{k_1}$$

Thus, one might assume that there exists a correlation between the property $\mu\sqrt{H}/k_1$ of a material and its relative hazard when in frictional contact with an explosive.

Dempster, arguing along the lines indicated above, showed that this was indeed the case for materials such as gunmetal, brass and steel, but aluminum gave too high a hazard value[15]. Dempster carried out his experiments with the help of a friction wheel. Gurton, Evans and Boyd carried out similar tests, for a large number of alloys, and when one examines their results, expressed in minimum speed of wheel turning to cause ignition of nitroglycerine, one finds a very good correlation (0.90) with the proposed relation, again with three aluminum alloys as exceptions[15]. More recently, Dempster has tested an additional 50 alloys in the same manner, and rated them in order of increasing hazard. The exceptional behavior of aluminum in most cases has been attributed to the chemical interaction between aluminum and the explosive's oxygen, thus giving a hotter "hot spot" and consequently faster expansion of this hot spot and greater ease of initiation.

At our laboratory, we carried out a number of hazard tests for purely frictional hazard, for 18 metallic and non-metallic materials. The friction wheel used (Figure 1) consists of a 10-12 in. disk of a material A to be chosen, which is turned by a two h.p., d.c. motor, the speed of which can be controlled by a Variac speed control box, whose settings correspond with speeds from 0-1700 r.p.m. The motor is bolted onto a rigid steel frame and a base which rests on hard rubber pads in order to keep vibration to a minimum. On the disk rests a rounded ¼-in. diameter pin of another material B, 4-5 in. from the centre of the shaft. The load on the pin can be varied from one ounce to five pounds. Diametrically opposite the pin a fine paint brush applies a few drops of the liquid explosive under investigation to the surface. On turning of the wheel the drops of explosive are smoothed out in a thin circular ring, which passes between the pin and the disk. The speed of the motor is increased slowly, until explosion occurs. Then the velocity of turning of the wheel is determined with a tachometer. This velocity (S) is indicative of the relative safety of the particular combination material A/explosive/material B chosen, a large velocity indicating a smaller degree of hazard.

Some of the results are presented in Table 1. The correlation between minimum velocity and $\frac{\mu \sqrt{H}}{k_1 + k_2}$ was, however, zero.

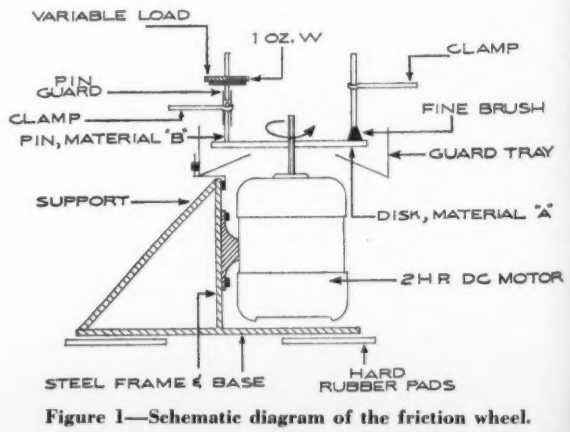

Figure 1—Schematic diagram of the friction wheel.

TABLE 1

A COMPARISON OF PHYSICAL PROPERTIES AND HAZARDS OF VARIOUS MATERIALS AS DETERMINED BY FRICTION WHEEL TESTS

A. Combination: Material (pin) — Stainless Steel (disk)

Material	$\frac{\mu\sqrt{H}}{k_1 + k_2}$	S(cm./sec.)
Glass	9.3	2.9
Stainless steel	8.3	6.5
Mild steel	7.6	4.7
Brass	5.3	4.1
Al-57SF	3.7	7.2
Al-54SB	2.8	5.2
Al-65ST-6	2.7	6.0
Al-1SF	1.3	5.4
Al-2S1/2H	1.3	6.0

B. Combination: Brass (pin) — Material (disk)

Material	$\frac{\mu\sqrt{H}}{k_1 + k_2}$	$\frac{S}{\text{(cm./sec.)}}$
Cupro-nickel	5.9	8.5
Stainless steel	5.3	17.2
Brass I	4.9	15.5
Al-57S1/2H	4.8	6.2
Al-57SF	4.8	8.4
Al-65ST-6	4.3	6.0
Brass III	4.3	12.6
Al-24ST-3	3.2	11.7
Al-54SB	1.9	7.4
Al-1SF	1.7	6.0
Bakelite	6.5	>32
Maple	2.0	>32
Fir	2.2	>32

The explanation of this behavior probably lies in the false assumption of constancy of the properties μ, H and k as friction is progressing. As the pin slides over the disk, abrasion of the disk occurs, and μ, H and k will change. However, repeated runs over the same area of contact, still yielded reproducible minimum velocity values.

In view of these experiments, a pendulum apparatus such as described by Bowden and Yoffe[11] is probably preferable for measurements of pure frictional hazards, since there the temperature increase is almost instantaneous, and complications such as bulk heating and abrasion would not arise. The pendulum apparatus might be approximated by using a friction wheel with short tests of one or two seconds duration.

In accidental mishaps, such as when a hammer drops on an explosive soiled floor, the hazard can best be tested by means of an apparatus simulating glancing blows. The torpedo frictional impact tester has found world wide application for this prupose. The apparatus, illustrated in Figure 2, consists of a brass V-shaped trough along an 8.7 lb. steel torpedo with a nose hardened to 700 Brinell, can slide down a small anvil made of the material under investigation. The small square of material is clamped into a steel base plate which rests on a concrete pad. The trough is inclined under a variable angle, usually 45°. A small amount of explosive is put on the surface of the anvil and covered with a standard type sandpaper. The torpedo is then caused to slide down on to the sample from varying fall heights, and the 50% explosion point is determined (h_s).

Some of the test results are presented as semi-logarithmic plots in Figures 3, 4 and 5. The values of h_s plotted in Figures 3, 4 and 5 are quite reproducible. Usually, values are within 0.2 inches from the average value given, and the maximum deviation obtained is ±0.5 inches.

One observes that, within the group of aluminum alloys, the relation $\mu\sqrt{H}/k$ correlates very well with the vertical fall

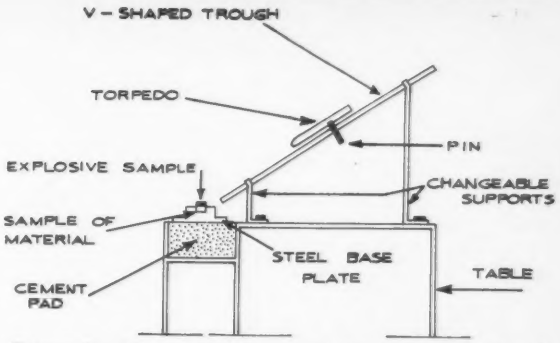

Figure 2—Schematic diagram of the torpedo frictional impact tester.

height value, for PETN (penta-erythritol-tetranitrate), R-NG (regular nitroglycerine) and for 75G-NG, which is a nitrated mixture of 75% ethylene glycol and 25% glycerol. All three explosives used were commercial grades. No attempts were made to purify the materials, since it was thought desirable to test the explosives that are actually being used in an explosives plant.

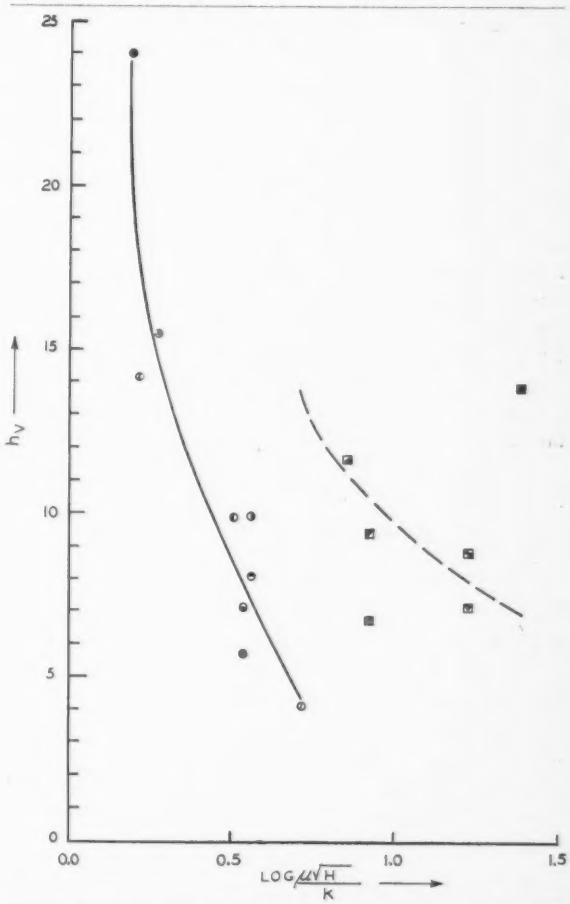

Figure 3—Comparison of physical properties and hazards of various materials in contact with *PETN*, as determined by torpedo friction tests. The circles denote aluminum alloys, viz.:

● 1*SF*; ⊙ 50*SF*; ◕ 2*S*-1/2*H*; ◐ 57*S*-1/2*H*; ◑ *B*54*S*; ◓ 24*ST*-3; ◒ 65*ST*-6; ⊗ 57*SF*; ∅ 17*ST*-4.

The squares denote other metals, viz.:

◪ Brass III; ■ Cupro-nickel; ◩ Brass II; ◪ Nickel; ◪ Brass I; ▽ Steel.

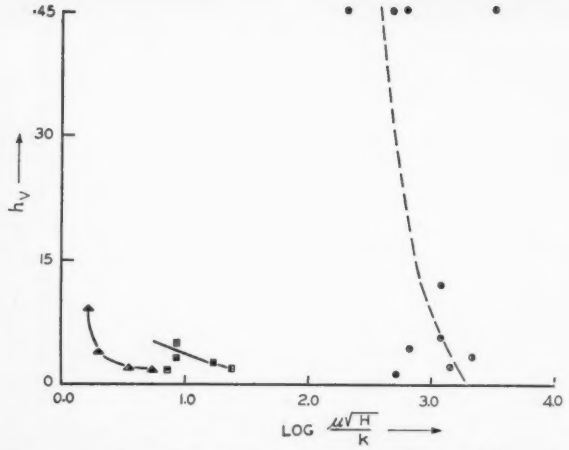

Figure 4—Comparison of physical properties and hazards of various materials in contact with *R-NG*, as determined by torpedo friction tests. The symbols denote:
△ Al 2S-1/2*H*; ▲ Al 50 *SF*; ▲ Al 65 *ST*-6; ▲ Al 17 *ST*-4; ▬ Brass III; ◪ Brass II; ⊡ Brass I; ▬ Steel and Nickel; ◧ Cupro-nickel; ● Teflon; ⊙ Maple; ◒ Oak; ◐ Masonite; ◍ Painted steel; ⊗ Transite; ⌀ Bakelite; ◓ Nylon; ◓ Hard rubber; ◑ Tufnol.

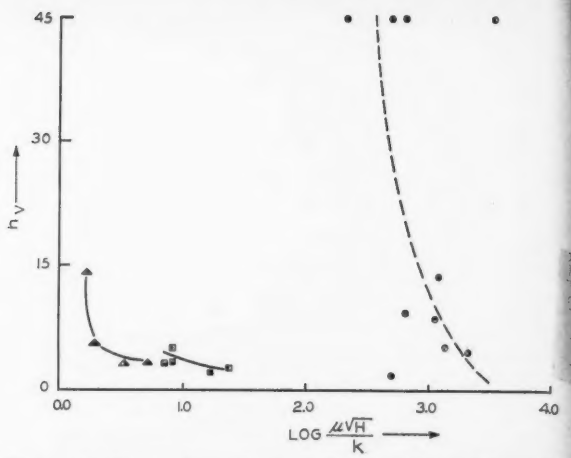

Figure 5—Comparison of physical properties and hazards of various materials in contact with *75G-NG*, as determined by torpedo friction tests. The same symbols are used as in Figure 4.

Within the group of other metals, the correlation is poor in Figure 3, and fair in Figures 4 and 5. In Figure 3 a dashed line instead of a solid one is used to express the uncertainty. It is interesting to notice the reversed positioning of cupro-nickel and brass I in Figure 3, and in Figures 4 and 5. When PETN is used cupro-nickel is the safest of the non-aluminum alloys and brass I is the worst. However, with R-NG and 75G-NG, brass I is the safest and cupro-nickel almost the worst. This type of behavior was also noticed by Corbett, of African Explosives and Chemical Industries[16]. One observes from Figures 3, 4 and 5 that, although aluminum alloys are more hazardous than expected from their function $\mu\sqrt{H}/k$, several of them are still safer to use than, say, brass, e.g. Al 1 SF.

For non-metallic materials (see Figures 4 and 5) the correlation is poor, mainly because of two materials: painted steel and masonite. In the case of painted steel, the exceptionally low value of the vertical fall height indicates a large hazard, larger even than for ordinary steel. It is thought that here the paint film is broken and that the hardness of the steel itself, combined with the low thermal conductance of the paint creates the high temperature which is thought to be responsible for the hazard. The behavior of the masonite stands still unexplained.

Thus, although some of the test results can be explained with the theory based on the influence of physical material properties, predictions still appear to be largely unsatisfactory.

Thermal Hazards

In this category one need only consider the flammability of materials of construction, e.g., when several parts of the machinery are subject to continued friction, and one part inflames, the flame may propagate to parts in contact with the explosive. From this point of view, wood, although an ideal material to use from the point of view of sparks, friction or impact (see above), constitutes a real hazard. Fortunately, this hazardous situation arises from a very slow process, which can usually be detected in reasonable time by the machine operator.

Nomenclature

ΔT = temperature increment caused by friction, degrees C.
μ = coefficient of kinetic friction, dimensionless.
W = load between two surfaces, dynes.
v = velocity of sliding of two materials over each other, cm./sec.
a = radius of circular regions of contact between two materials, cm.
J = mechanical heat equivalent: 1 cal. = 4.18×10^7 ergs.
k = thermal conductivity of material, cal./cm. sec. degrees C.
H = hardness of material, Brinell hardness units.
p_m = yield pressure of material, kg./mm.^{2}
S = linear velocity of rotation of friction wheel, cm./sec.
h_v = vertical fall height in torpedo tests, inches.

References

(1) Braid, P. E., Langille, R. C., and Armstrong, A. M., Can. J. Technol. **34,** 45 (1956).
(2) Brown, F. W., Kusler, D. J., and Gibson, F. C., U.S. Bur. Mines, Rep. 3852 (1946) and 5002 (1953).
(3) Basset, J., and Basset, J., Compt. Rend. Acad. Sci. (Paris), **231,** 759 (1950).
(4) Rowlinson, H. C., C-I-L unpublished information.
(5) Henry, H. S., Brit. J. Appl. Phys., **4,** 41 (1953).
(6) Rowlinson, H. C., private communication.
(7) Morris, G., Engineering, **167,** 49, 73 (1947).
(8) Taylor, W., and Weale, A., Proc. Roy. Soc., **A138,** 92 (1932).
(9) Taylor, W., and Weale, A., Trans. Faraday Soc., **34,** 995 (1938).
(10) Wöhler, L., and Wenzelberg, O., Angew. Chemie, **46,** 173 (1933).
(11) Bowden, F. P., and Yoffe, A. D., "Initiation and Growth of Explosion in Liquids and Solids" (at the Univ. Press, Cambridge, 1952).
(12) Ivany, W. G., C-I-L unpublished information.
(13) Bowden, F. P., and Tabor, D., "The Friction and Lubrication of Solids" (at the Clarendon Press, Oxford, 1950).
(14) Bowden, F. P., Stone, M. A., and Tudor, G. K., Proc. Roy. Soc., **A188,** 329 (1947).
(15) I. C. I. unpublished information.
(16) Private communication from W. A. Caldwell.

★ ★ ★